170
110

Long-Term Thermal/Chemical Degradation of Ceramic Candle Filter Materials

by

Jean P. Miller

Thesis submitted to the Faculty of the

Virginia Polytechnic Institute and State University

in partial fulfillment of the requirements for the degree of

Master of Science

in

Materials Engineering

APPROVED:

Jesse J. Brown, Jr., Chairman

Jack L. Lytton

William T. Reynolds

May 1991
Blacksburg, Virginia

Long-Term Thermal/Chemical Degradation of Ceramic Candle Filter Materials

by

Jean P. Miller

Jesse, J. Brown, Jr., Chairman

Materials Engineering

(ABSTRACT)

Commercial ceramic candle filters were exposed to harsh environments to determine the effects of alkali and steam on their long-term durability. Ceramic candle filters are composed of relatively coarse aggregates fixed by a ceramic bond. The filters studied include a clay-bonded, granular aluminosilicate candle and three types of clay-bonded, granular SiC candles. The alkali, steam, and steam-alkali corrosion of these commercial ceramic candle filters was examined at temperatures ranging from 450 to 1225°C and pressures up to 1000 psi. Results indicate that the aluminosilicate candle filters perform better than filters made from granular SiC. The SiC filters show binder degradation in steam as well as in alkali-containing environments at temperatures as low as 700°C, with oxidation of the SiC occurring in the steam environments at higher temperatures. Sodium and potassium contaminants in the steam atmospheres accelerate the degradation of both types of filter material.

Acknowledgements

I would like to express my sincere appreciation to my advisor, Dr. Jesse J. Brown, Jr., for his help and guidance in my graduate studies and for the opportunity to work at the Center for Advanced Ceramic Materials. I would like to thank Nancy Brown for her guidance on this research project as well as her editorial assistance on monthly progress reports. I would also like to thank my committee members, Dr. Jack L. Lytton and Dr. William T. Reynolds.

In addition, I would like to express my gratitude to the following people:

Ruth Hallman for her encouragement and concern for my emotional and physical well-being.

Bob Hallman for his assistance in setting up lab equipment.

Tawei Sun for his advice concerning this research.

Colleagues Steve Van Aken, Laurent Battu, K.H. Lee, and Yaping Yang for making me laugh.

Sandra Ganzalez, my office-mate and good friend who has been with me through thick and thin.

Finally and most importantly, I wish to thank my parents Jake and Daphne Miller, without whose support and understanding all this would not be possible.

Table of Contents

1. Introduction 1

2. Literature Review 2

3. Experimental Procedure 14

3.1 Exposure to Alkali 19
3.2 Exposure to High Pressure Steam 19
3.3 Exposure to High Pressure Steam and Alkali 20
3.4 Sample Evaluation 23

4. Results and Discussion 25

4.1 Granular Aluminosilicate 25
4.2 Granular SiC 30
4.3 Layered SiC 41
4.4 Membrane SiC 46
4.5 Comparison of Filters 54

5. Conclusions 56

6. References 57

7. Vita 60

List of Figures

Figure 1. Schematic of candle filter module illustrating a series of candles supported by a tubesheet with direction of dirty gas flow and pulse air cleaning 4

Figure 2. Sources of stresses in a candle filter 6

Figure 3. SEM micrograph of clay-bonded granular aluminosilicate candle filter. (100X) 15

Figure 4. SEM micrograph of clay-bonded granular SiC filter with a uniform aggregate size. (200X) 16

Figure 5. SEM micrograph of clay bonded granular SiC filter with an outer layer of small aggregates. Micrograph shows boundary between the two layers of aggregates. (150X) 17

Figure 6. SEM micrograph of clay-bonded granular SiC filter with a fibrous membrane on the filtration surface. (100X) 18

Figure 7. Hydrothermal furnace set-up 21

Figure 8. Schematic showing position of layered SiC filter specimen in platinum test chamber 22

Figure 9. Schematic showing sectioning and mounting of filter specimens 24

Figure 10. SEM micrograph of clay-bonded, granular aluminosilicate filter exposed to steam at 1000°C for 24 h at 200 psi. (330X) 26

Figure 11. SEM micrograph of clay-bonded granular aluminosilicate filter exposed to steam and NaOH at 800°C for 24 h at 200 psi. (2000X) 28

Figure 12. SEM micrograph of clay-bonded granular aluminosilicate filter exposed to NaOH and steam at 1000°C for 24 h and a pressure of 500 psi. (200X)..... 29

Figure 13. Comparison of as-received and alkali-soaked granular SiC filter. (A) As-received granular SiC filter specimen, (B) granular SiC filter soaked in sodium, dried, and fired at 1000°C for 12 h.....31

Figure 14. SEM micrograph of granular SiC filter soaked in NaOH, dried, and fired at 925°C for 12 h. (200X)..... 32

Figure 15. Comparison of as-received and alkali-soaked granular SiC filter. (A) As-received granular SiC filter specimen, (B)granular SiC filter specimen exposed to 2:1 mixture of KOH and NaOH for 12 h at 1000°C..... 33

Figure 16. SEM micrograph of layered SiC filter soaked in a 2:1 mixture of KOH and NaOH, dried, and fired at 700°C for 12 h. (200X)..... 34

Figure 17. Arrangement of SiC filter specimens and kaolinite bars in furnace. (A) Exposed membrane SiC filter (top) and exposed granular SiC filter (bottom), (B) crucible containing K_2CO_3, (C) exposed kaolinite bar with glazed surface. Exposure conditions: K_2CO_3 at 1225°C for 20 h..... 35

Figure 18. SEM micrograph of interior section of clay-bonded granular SiC filter exposed to KOH and steam at 900°C for 24 h at 200 psi. (200X)..... 39

Figure 19. SEM micrograph of exterior section of clay-bonded granular SiC filter exposed to KOH and steam at 800°C for 24 h at 200 psi. (200X)..... 40

Figure 20. Comparison of as-received and alkali-soaked layered SiC filter. (A) layered SiC filter specimen soaked in sodium, dried, and fired at 700°C for 12 h. Note severe volume expansion in smaller grained area, (B) As-received granular SiC filter with an outer layer of small aggregates.....42

Figure 21. Low magnification SEM micrograph of granular SiC filter soaked in sodium, dried, and fired at 1000°C for 12 h. (20X)..... 43

Figure 22. SEM micrograph of small aggregates on outer surface layered, granular SiC filter exposed to NaOH and steam at 700°C for 24 h at 500 psi. (500X)..... 45

Figure 23. SEM micrograph of outer surface of membrane SiC filter after exposure to K_2CO_3 vapors for 24 h. (200X).....48

Figure 24. SEM micrograph of interior section of membrane SiC filter after exposure to K_2CO_3 vapors at 1225°C for 24 h. (100X)..... 49

Figure 25. SEM micrograph of membrane SiC filter exposed to steam at 900°C for 24 h at 200 psi. (200X)..... 50

Figure 26. SEM micrograph of the membrane SiC filter exposed to NaOH and steam at 800°C for 24 h at 200 psi. Note the formation of cristobalite beads. (2000X)..... 53

1. Introduction

Coal is our most abundant energy resource, but constitutes very little of the nationally consumed energy. Coal represents an enormous resource which must be more effectively utilized. Combined cycle power generation is an advanced coal conversion process which utilizes coal in an energy efficient and environmentally sound manner. Combined cycle plants can combust coal in pressurized fluidized bed combustors (oxidizing atmosphere) or gasify coal in gasification combined cycles (reducing atmosphere) in a number of technologies under development. One of the constraints to the utilization of combined cycle systems is the clean-up of the hot gas prior to use in gas turbines. Removal of gaseous and particulate contaminants from gas streams at high temperatures is essential for cost-effective operation of advanced coal combustion processes. Thus, the term hot gas clean-up was adopted. Cleaning of hot gases requires a device capable of operating at high temperatures and pressures (590 - 1000°C and 150 - 450 psi). Conventional gas cleaning technologies which require that the gas be cooled prior to filtration have been used in industry for several years. These devices include cyclones, fabric filters, scrubbers, and electrostatic precipitators, but their overall performance is deficient due to reduced system efficiency from gas cooling and poor

particulate removal efficiencies of only 65-70%.

Control and removal of contaminants in the gas stream, therefore, constitute a required step in advanced coal conversion processes. Sulfur particulate and alkali compounds are the most frequently observed contaminants in coal conversion environments. High concentrations of steam (30-50%) are also present in advanced coal conversion environments. Alkali contaminants can cause hot corrosion leading to catastrophic failure in turbine components; therefore, the alkali content in coal combustion gases must be controlled. High temperature ceramic candle filters are promising devices for the removal of ash and alkali-containing compounds, yet they have exhibited only short-term durability due to a combination of mechanical, thermal, and chemical failures. The current high failure rate of these candle filters is unacceptable for commercial applications due to the potential economic cost of damaged turbine components, environmental hazards, and system down time.

In view of the poor performance of the high temperature candle filters, there remains a need for a better understanding of contaminant-filter interactions at operating temperatures and pressures of coal combustors and gasifiers. The goal of this research was to study the reactions of alkali and steam with commercial candle filter materials.

2. Literature Review

Ceramic Candle Filters for Hot Gas Clean-up

Candle filters are made by bonding ceramic fibers or grains to form a porous, hollow cylinder approximately 8 cm in diameter and 1 to 1.5 m in length.[1] The wall thickness of the candles ranges from 1 to 1.5 cm. Most commercial candle filters are made using SiC or aluminosilicate aggregates fixed by a ceramic bond. Some candles incorporate fibers or fine grains to form a membrane on the filtration surface. Candle filters have exhibited collection efficiencies of 99% and are much stronger than woven ceramic fabrics, but have the drawback of low porosity and consequent high pressure drop across the filter wall during operation.[1] Figure 1 illustrates the general principle of candle filter operation. The steel chamber houses several stages providing 50-100 candles in each. Gas laden with particulates enters the chamber which contains a series of candle filters supported by a metal tube sheet. Particulates are trapped on the outside of the candle filter as hot gas passes through the filter system. As particulates accumulate, an ash cake forms which actually becomes a filtering mechanism at the initial stage. Cleaning the filters involves removing the ash cake by jet pulsing clean air through the filter in the reverse

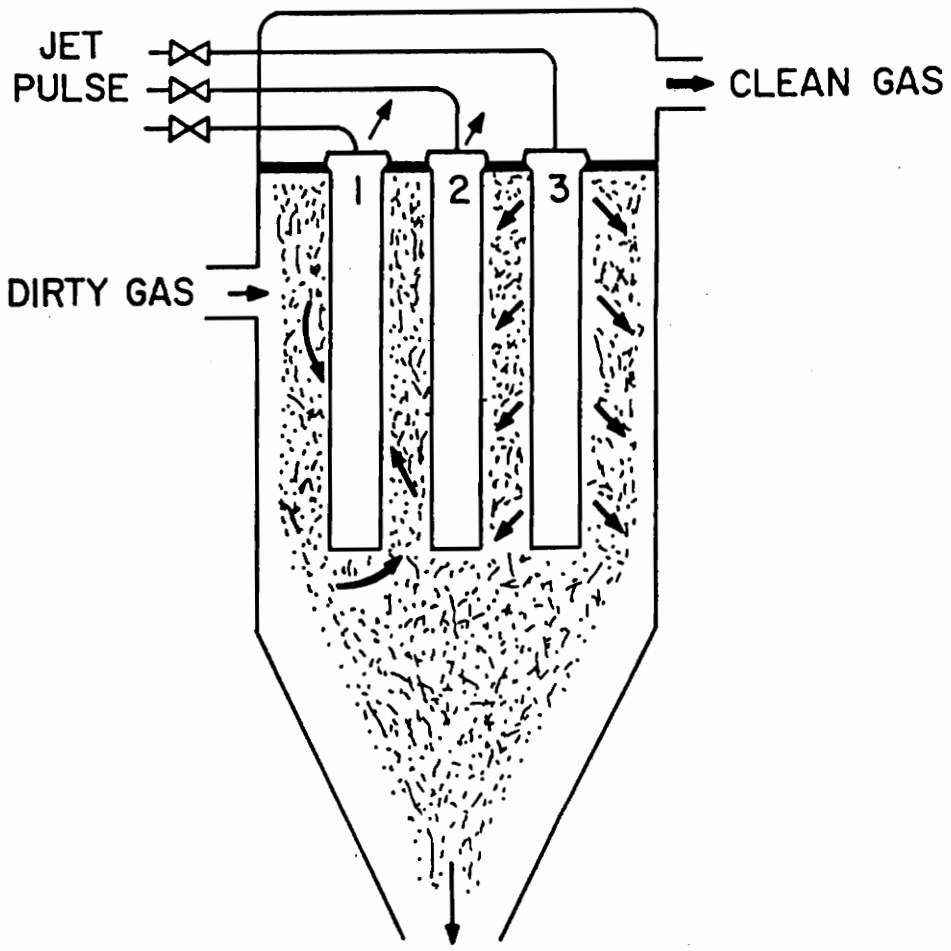

Figure 1. Schematic of candle filter module illustrating a series of candles supported by a tubesheet with direction of dirty gas flow and pulse air cleaning.

direction of the gas flow. Depending on the system, filters are pulsed 3-20 times per hour. Fallen ash cakes are then removed through the bottom of the chamber.

Most candle filter failures occur in the first several hundred hours of operation due to mechanical or thermal stresses. Chemical and thermochemical effects in the long run may also reduce the durability of these filters.[2] A number of commercially available ceramic materials have adequate temperature resistance for hot-gas cleaning conditions. However, a problem arises with the introduction of a binder having inferior refractory properties. Generally, refractory materials are considered chemically inert, but ceramics may become prone to chemical degradation when placed in a high temperature environment containing corrosive species. Several corrodants have been identified which lead to the chemical degradation of the binder material in candle filters including alkali, steam, carbon monoxide, hydrogen, and iron oxide. Corrosion of the filter by alkali-containing ash and gases causes compositional changes which result in high thermally expanding crystalline phases. These phases leave the filter prone to thermal shock. Thermal shock also occurs during start-up and shut-down and pulse cleaning.

As well as temperature and corrosion resistance these materials must also have sufficient strength to resist the mechanical stresses induced during operation. Mechanical problems have been experienced and are associated with cracking of the candles especially near the flange due to excessive mechanical and thermal stresses during operation.[1,3] Since the candle filters must only support their own weight plus the weight of the dustcake, the strength required by the filters is relatively low. However, they must be able to withstand mechanical stresses created by process vibrations, handling, cleaning, and clamping arrangements. Figure 2 illustrates the sources of stresses in a candle filter element. Repeated filtering and cleaning cycles result in alternating compressive and tensile stresses

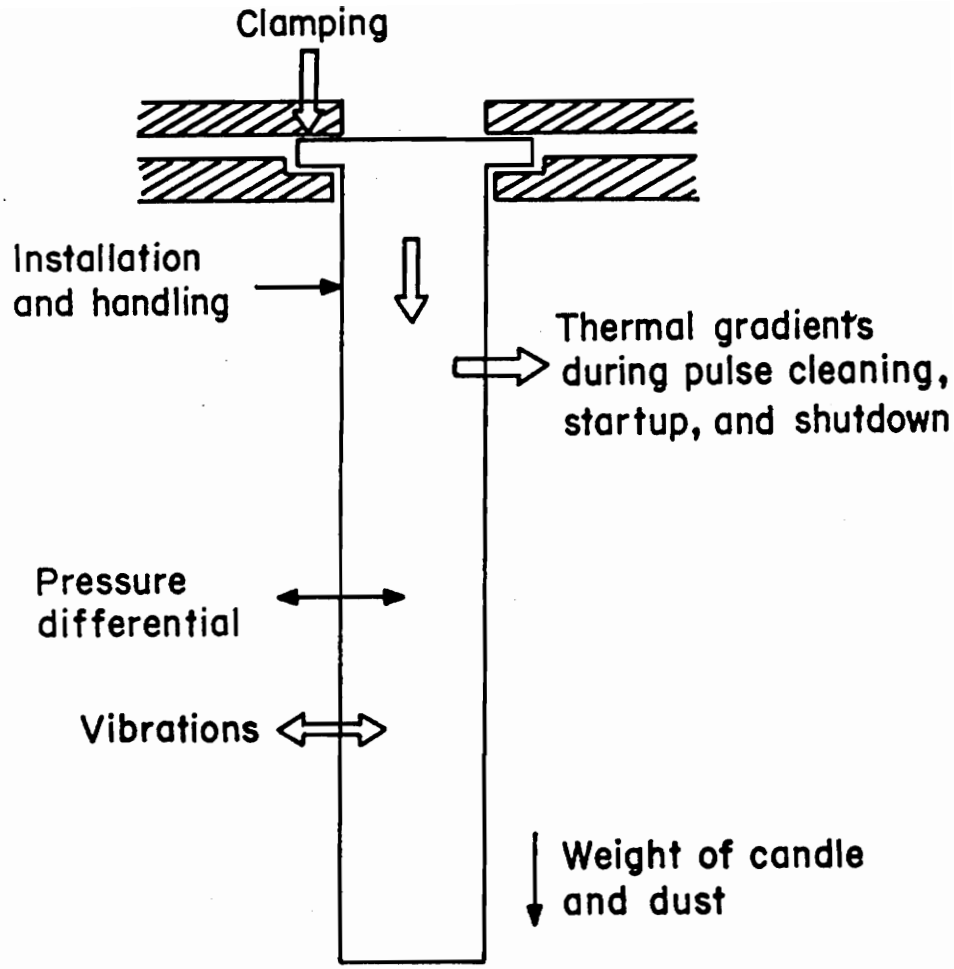

Figure 2. Sources of stresses in a candle filter.

which may cause cyclic fatigue. Since ceramics are susceptible to brittle fracture these mechanical stresses must be controlled. It has also become a concern that particulate collected on the surface of the filter may eventually plug the pathways across the filter.

Chemical Attack of Aluminosilicate Ceramics

The corrosion of aluminosilicate materials by alkali compounds has been studied thoroughly. Refractory materials are subject to chemical and microstructural degradation associated with prolonged contact with a number of alkali compounds such as oxides, hydroxides, and carbonates of potassium and/or sodium.[5] A typical reaction proposed by Kennedy [6] is shown below:

$$11(Al_6Si_2O_{13}) + 26(NaOH) \longrightarrow 22(NaAlSiO_4) + 4(NaAl_{11}O_{17}) + 13H_2O$$

The resulting products in this reaction cause a 30% volume expansion which leads to cracking, bloating, and spalling of the material. Similar reactions occur with potassium compounds. Dierks and Stahl [5] determined that alkali attack is a long-term failure mode for refractories, and that medium-alumina refractories prove to be the most resistant to alkali failure.

Hayden [7] studied the reactions of alkali vapors with various aluminosilicate (19-99% Al_2O_3) refractories. She found that resistance to alkali attack increases with increasing alumina content. Aluminosilicate refractories exhibit increased resistance to alkali with Al_2O_3 contents up to 60%, but further increases of alumina content above 60% did not increase resistance to alkali attack. Hayden attributed the resistance to alkali attack of aluminosilicates containing 60% or less alumina to reactions which form a glassy phase on

the surface and seal the ceramic surface, preventing deeper penetration of alkali compounds. Aluminosilicates with greater than 60% alumina did not have this surface sealing reaction and are prone to expansive reactions which form alkali compounds on the surface resulting in subsequent disintegration. The surface layer of aluminosilicate refractories (>60% Al_2O_3) exposed to sodium-containing environments consisted of nephelite, sodium alumino-silicate, sodium beta-alumina, and sodium aluminate. The growth of these products led to the separation of the layers from the refractory, thereby exposing inner surfaces of the brick to alkali attack. This separating effect may be attributed to the greater specific volume of these soda-containing phases in comparison to the unexposed refractory materials. Similar results were encountered with potassia vapor reaction with the formation of the phases leucite and/or kaliophilite, orthorhombic $KAlSiO_4$, potassium beta-alumina, and potassium aluminate. These expansive reactions can cause spalling leading to catastrophic failure.

Farris and Allen [8] have investigated alkali reactions with aluminosilicate refractory materials ranging from 42-90% Al_2O_3 using K_2CO_3 and Na_2CO_3. Reactions between the aluminosilicate material and the K_2CO_3 were found to occur at temperatures as low as 590°C. Reactions between the potassium oxide and the refractories were found to form potassium aluminum silicates at low temperatures, and potassium aluminates at temperatures above 1100°C. Similar reactions occurred with sodium oxide resulting in the formation of sodium aluminum silicates at low temperatures and sodium aluminates at temperatures above 1100°C. These researchers concluded that refractories containing 42-70% alumina have the greatest resistance to alkali attack with the 42% alumina refractory performing significantly better than the 70% alumina material. The superior alkali resistance of the 42% alumina refractory was attributed to the ability of the silica phase to

react more rapidly with the alkali and contain its attack on the surface.

Rigby and Hutton [9] have shown that alumina-containing refractories with a composition of 40% alumina and 60% silica can react with alkali to form a liquid at 1000°C. They also found that refractories with higher alumina content suffer severe volume expansion after exposure to alkali compounds. This volume expansion was attributed to the formation of sodium aluminate, a lower density material. As alumina content increased to 75%, the degree of refractory bloating increased.

Wei et al. [10] studied the effects of coal combustion environments on 37% alumina refractories. Exposed sides of bricks consisted of a glassy phase with crystals of a sodium/calcium/aluminum silicate and a high concentration of alkali. Other phases included corundum, mullite, and cristobalite. This glassy surface formed when alkali reacted with free silica to form low melting eutectics. As the reaction proceeded, the surface glassy phase continued to dissolve free silica. Wei et al. also found that mullite is attacked and dissociates into corundum and more free silica. The glassy phase actually protects the refractory brick from further degradation as long as its viscosity remains high. They determined that 37% alumina fireclay refractories are suitable for applications at temperatures below 1260°C.

Havranek [11] studied alkali attack of several refractories including aluminosilicates (45-90% alumina). Hot modulus of rupture data were obtained at different temperatures for refractory bars exposed to molten potassium carbonate in a reducing atmosphere. Their test results showed that mullite-bonded alumina maintained good strength after alkali attack at 1400°C, whereas refractories with low porosity and excess silica glass maintained good strength only at 1250°C. Havranek also suggested the following reactions for aluminosilicate refractories exposed to alkali in reducing atmospheres:

Fireclay: $4K + 2/3(3Al_2O_3 \cdot 2SiO_2) + 8/3\ SiO_2 + 2CO \rightarrow 2(K_2O \cdot Al_2O_3 \cdot 2SiO_2) + 2C$ or

(kaliophilite)

$2(K_2O \cdot Al_2O_3 \cdot 4SiO_2) + 2C$

(leucite)

Mullite: $8K + 3Al_2O_3 \cdot 2SiO_2 + 4CO \rightarrow 2(K_2O \cdot Al_2O_3 \cdot 2SiO_2) + 2Al_2O_3 \cdot K_2O + 4C$

Alumina: $2K + 11Al_2O_3 + CO \rightarrow K_2O \cdot 11Al_2O_3 + C$

(ß-alumina)

The alkali reactions with fireclay involve a 6% volumetric expansion for kaliophilite formation and a 10% expansion for leucite formation. Alkali reactions with mullite and alumina result in 15% and 17% expansions, respectively.

Chemical Attack of Silicon-Containing Ceramics

The oxidation resistance of SiC relies on the protective oxide layer formed on the surface which effectively inhibits further oxidation. The stability of this silica layer then becomes the key to whether or not further attack may occur. [12,13]

SiC and Si exhibit two types of oxidation behavior.[13,14,15] At relatively low oxygen partial pressures, SiC and Si exhibit active oxidation behavior according to the reactions:

$$SiC + O_2 \text{ ---> } SiO + CO$$

$$2Si + O_2 \text{ ---> } 2SiO$$

In both cases, only gaseous reaction products form and both materials experience a continuous weight loss as oxidation takes place. As the oxidation of the system increases, a transition to passive oxidation behavior occurs. This transition is temperature dependent. The passive oxidation reactions are given by the following equations:

$$2SiC + 3O_2 \text{ ---> } 2SiO_2 + 2CO$$

$$Si + O_2 \text{ ---> } SiO_2$$

In the case of passive oxidation, a silica film is formed on the surface of SiC, which tends to inhibit further oxidation.

Fox et al.[16] studied the hot corrosion of silicon carbide following experiments in which commercially available SiC was exposed to a simulated turbine environment containing sodium chloride at various temperatures. Samples of SiC were coated with Na_2SiO_4 by spraying heated specimens with a saturated salt solution and suspended in a vertical tube furnace in a flowing oxygen atmosphere. Fox et al. found that corrosion occurred at temperatures as low as 850°C. At 1000°C a more accelerated attack occurred that involved the oxidation of the carbide and the formation of sodium silicate by the following reactions:

$$SiC + 3/2\ O_2 \text{ ---> } SiO_2 + CO$$

$$xSiO_2 + Na_2SO_4 \text{ ---> } Na_2O{\cdot}x(SiO_2) + SO_3$$

The evolution of CO and SO_3 produced bubbles in the SiC samples. Observation of the exposed surfaces revealed the presence of a glassy corrosion product which contained large bubbles. The mechanism of corrosion was determined to be a continuous process involving the oxidation of SiC and the dissolution of SiO_2 to form a liquid phase of $Na_2O{\bullet}x(SiO_2)$. Upon removal of the glassy phase, extensive pitting was observed in the SiC. The sodium appeared to have caused significant damage to the protective silica layer, thus allowing oxygen to penetrate and react with the SiC.

Jacobson and Smialek [17] deposited thin films of molten Na_2SO_4 and Na_2CO_3 to corrode sintered SiC at 1000°C. They found that these films lead to glassy products on the SiC surface after 48 h at 1000°C. These products contained small amounts of sodium silicate and 10 to 20 times the amount of silica. The attack produced pitting due to gas evolution and grain boundary etching. Smialek, et al. [18] concluded that this type of corrosion causes significant strength degradation ranging from 15-50% depending on the specific material and exposure condition.

Crowley's [19] work on silica-containing refractories indicates that silica volatilization is a significant problem in high pressure atmospheres containing dry H_2 and H_2-steam. He suggested that the following reaction is responsible for weight loss through SiO volatilization above 1150°C:

$$SiO_2 + H_2 \text{---> } SiO + H_2O$$

Dial [20] stated that steam can also cause silica volatilization, but suggested that the reaction product is H_2SiO_4. He concluded that refractories low in SiO_2 are necessary to resist steam attack.

Sadler et al.[21,22] examined high silica, alumina-containing refractories after exposure to steam at temperatures up to 1400°C and at steam partial pressures up to 1000 psig. They concluded that steam-induced silica losses from silica-alumina refractories are insignificant below 1000°C at steam partial pressures up to 1000 psig. However, Sadler et al. found that SiC refractories bloated or disintegrated in exposures to high pressure (1000 psig) steam-containing atmospheres at temperatures ranging from 760 to 980°C. Horn et al.[23] suggested that corrosion of SiC is caused by a two-step reaction where H_2O dissociates into oxygen and hydrogen, and the oxygen reacts with SiC to form SiO_2. Both studies recommend against the use of SiC in steam-containing environments at temperatures above 1000°C.

Tressler at al.[24] found that water vapor greatly increased the rate of oxidation of SiC by acting as an oxidant at the reaction interface and reducing the viscosity of the SiO_2 layer by the presence of OH- ions. Federer [25] found that the lowered viscosity of SiO_2 coatings on SiC by reactions with alkali oxides and SiO_2 layer allows greater transport of oxygen through the layer and thus greater oxidation of the SiC.

3. Experimental Procedure

Four types of commercial candle filters were exposed to harsh environments in this investigation. These include a clay-bonded ***granular aluminosilicate*** filter with 100-200 μm aggregates and three types of clay-bonded SiC filters which can be distinguished by aggregate size and filtration surface characteristics. Of the three types of SiC filters, one candle filter has a uniform aggregate size ranging from 90 to 100 μm and will be denoted ***granular SiC***. Another SiC filter has an inner layer of aggregates ranging in size from 90 to 100 μm with a layer of smaller aggregates on the filtration surface, 20 - 30 μm in size. This filter type will be referred to as ***layered SiC***. The third SiC filter with aggregates ranging in size from 300-500 μm has an aluminosilicate fibrous membrane which coats the filtration surface, and will therefore be named ***membrane SiC***.

The morphology of the four types of as-received filters was examined using SEM for comparison between exposed and unexposed filters. Figure 3 shows the fracture surface of the as-received clay-bonded aluminosilicate filter. The granular, layered, and membrane SiC filter morphologies are shown in Figures 4, 5, and 6, respectively. EDX analysis of the aluminosilicate filter indicates an approximate aggregate composition of 26%

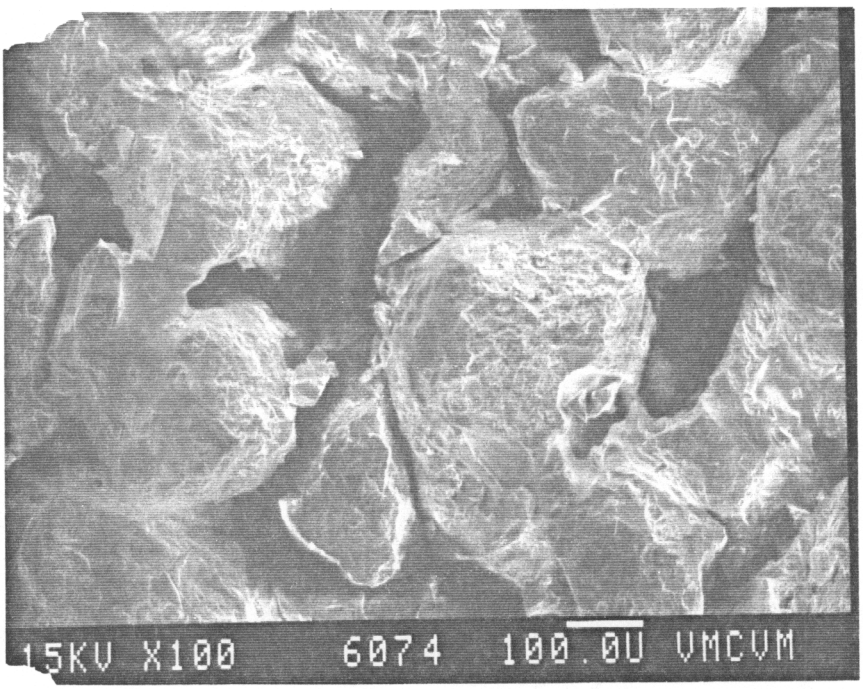

Figure 3. SEM micrograph of clay-bonded granular aluminosilicate candle filter. (100X)

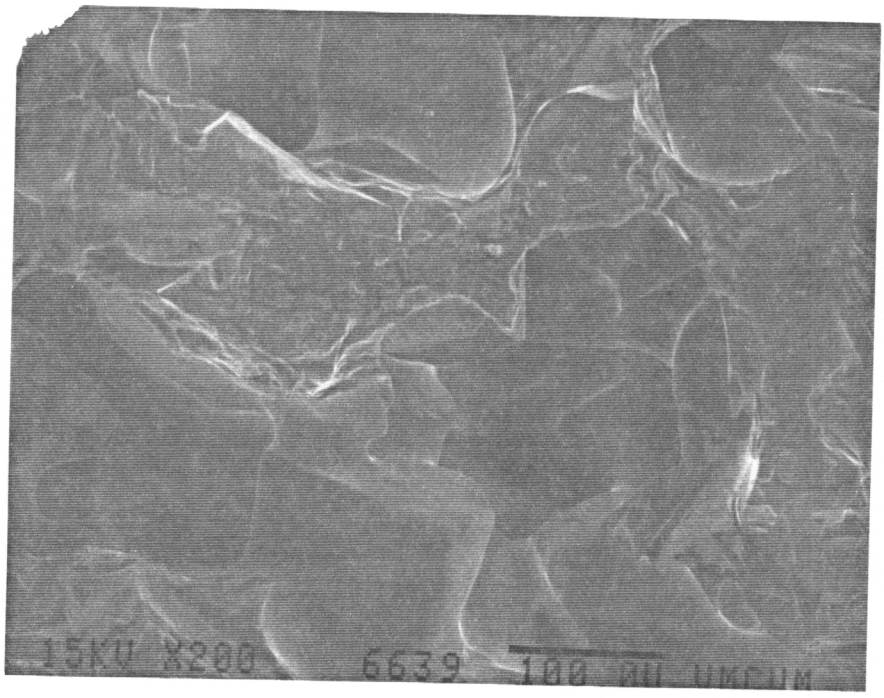

Figure 4. SEM micrograph of clay-bonded granular SiC filter with a uniform aggregate size. (200X)

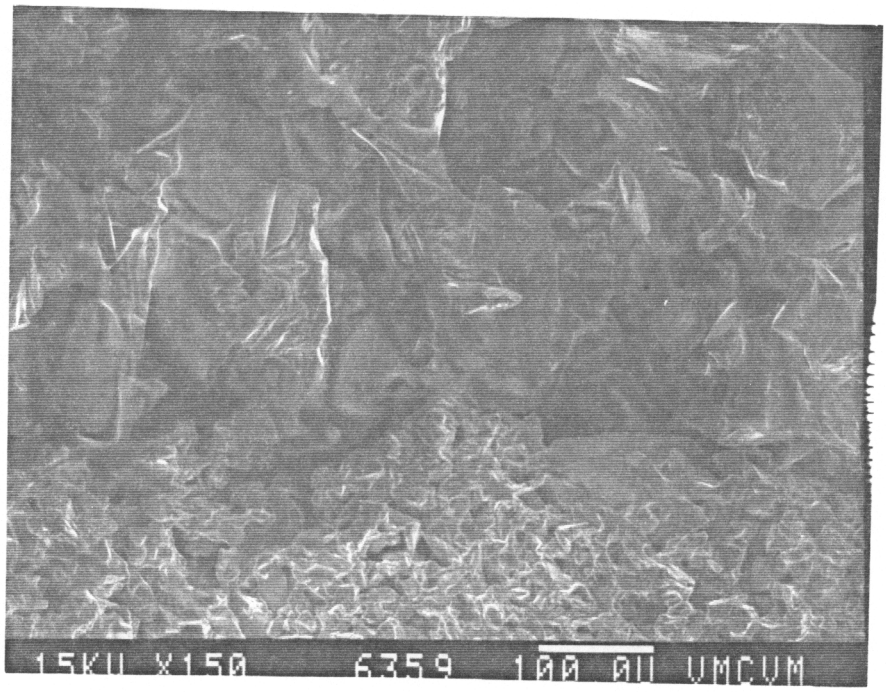

Figure 5. SEM micrograph of clay bonded granular SiC filter with an outer layer of small aggregates. Micrograph shows boundary between the two layers of aggregates. (150X)

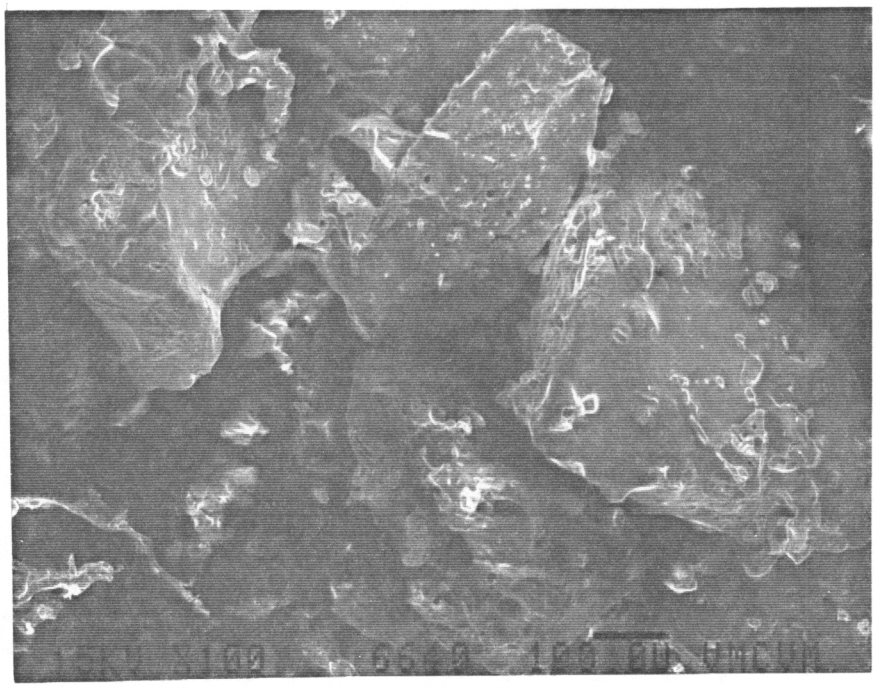

Figure 6. SEM micrograph of clay-bonded granular SiC filter with a fibrous membrane on the filtration surface. (100X)

Al_2O_3, 68% SiO_2, with small amounts of Fe_2O_3, TiO_2 and CaO, and a binder composition of 30% Al_2O_3, 68 % SiO_2, with trace amounts of CaO and TiO_2. EDX analysis of the SiC filters indicate alumina/silica bond compositions of 8% Al_2O_3 and 92% SiO_2 for the granular SiC; 13% Al_2O_3 and 87% SiO_2 for the layered SiC; and 17% Al_2O_3, 80% SiO_2, and 3% alkali for the membrane SiC filters.

3.1 Exposure to Alkali

Alkali tests were conducted on the granular, layered, and membrane SiC candle filters. Specimens of each filter with dimensions approximately 1x1x1 cm were soaked for 24 h in a saturated solution of NaOH or KOH and allowed to air dry. Experiments in which the filter specimens were soaked for 24 h in a saturated solution of both KOH and NaOH were also conducted. A 2:1 ratio of KOH to NaOH was made with 250 g KOH and 125 g NaOH in 300 mL of water. The alkali-impregnated samples were then placed in an alumina combustion boat and fired at temperatures ranging from 450 to 1000°C for up to 12 h.

The membrane and granular SiC candle filter specimens were fired at 925 and 1225°C for 6, 12, and 24 h in the presence of and equal distances from either 4 g Na_2CO_3 or 3 K_2CO_3 placed separately in a box furnace to provide an alkali source. It should be noted that the SiC samples were located approximately 2 cm from the alkali source and the membrane SiC filter was placed in an alumina combustion boat such that the outer fibrous membrane was exposed to the alkali vapor.

3.2 Exposure to High Pressure Steam

Exposures of the granular aluminosilicate, granular SiC, and layered SiC candle filters to high pressure steam were conducted in a hydrothermal furnace test unit. A schematic of the

unit is shown in Figure 7. Filter samples with dimensions approximately 3x3x15 mm were cut and sealed in a platinum tube (inner diameter 5 mm) containing the amount of H_2O required to generate steam atmospheres at the desired temperatures and pressures. The amount of H_2O necessary to generate the desired pressures was calculated using the ideal gas law and the volume of the platinum sample container. The sample container was placed in a pressure cell which was purged with argon gas. The argon was maintained at a pressure equal to the pressure within the sample tube to ensure that the sample container would not be subjected to stresses due to a high pressure differential. An inert backfill gas was used to preclude oxidation of the molybdenum-titanium alloy pressure vessel.

The filter samples were exposed to the steam environments at temperatures ranging from 700 to 1000°C and pressures of 200, 500, and 1000 psi. Filter samples were exposed to these conditions for 24 h. The sealed platinum tube containing the sample and H_2O was weighed before and after the exposure to ensure that the steam atmosphere was maintained and weight loss had not occurred.

3.3 Exposure to High Pressure Steam and Alkali

Tests were conducted to study the effects of alkali in a high pressure, steam-containing atmospheres on the four types of ceramic candle filters. Methods of hydrothermal exposure described above were used except that solutions of either 5 molar NaOH or 5 molar KOH were sealed in the platinum sample tube with the filter specimens. Special care was taken in positioning the layered SiC filter specimens in the platinum tubing to ensure comparable conditions for all exposure . The filter specimen and alkali solution were sealed in the tubing as shown in Figure 8, with the larger SiC grains positioned at the bottom of the tube. During

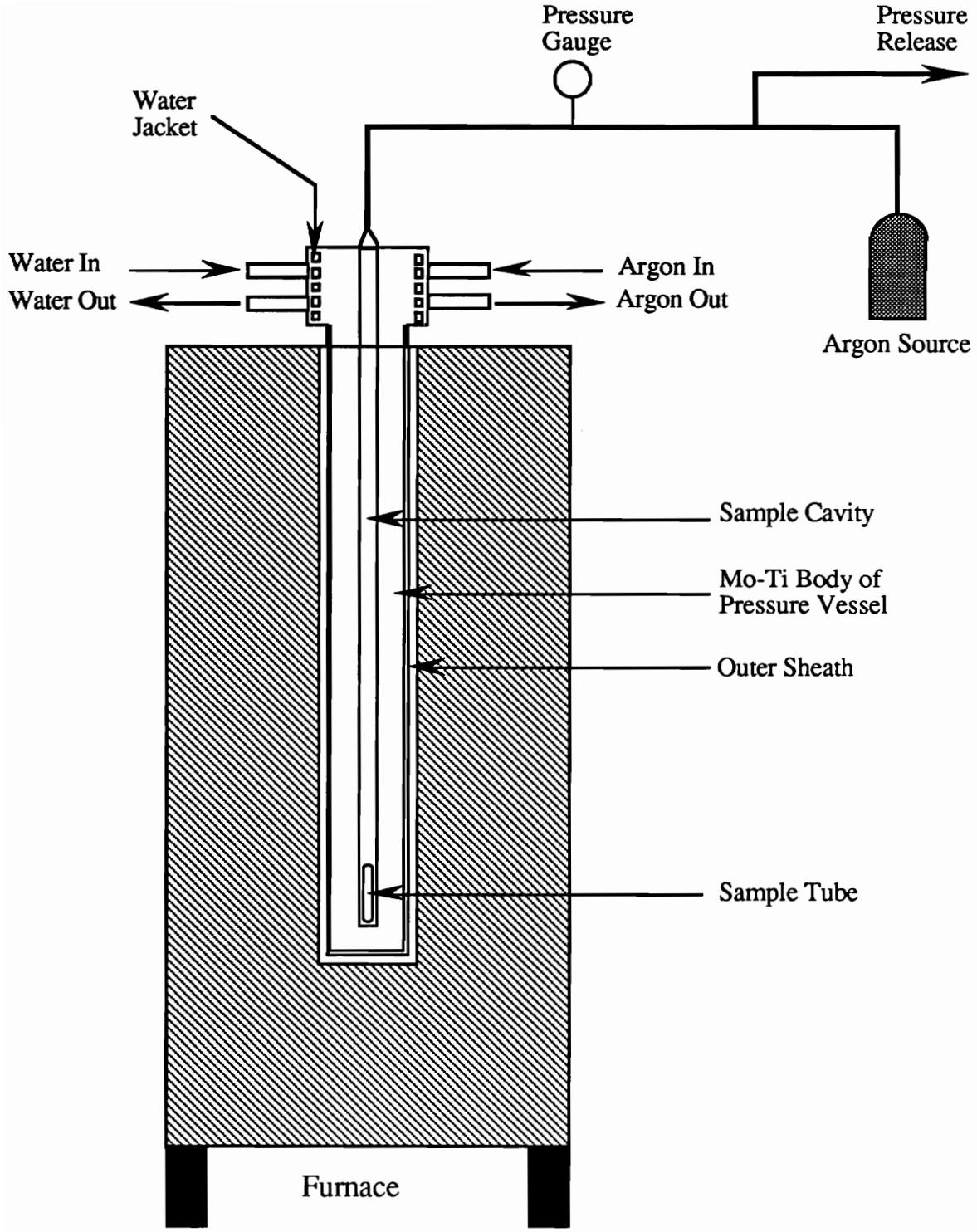

Figure 7. Hydrothermal furnace set-up.

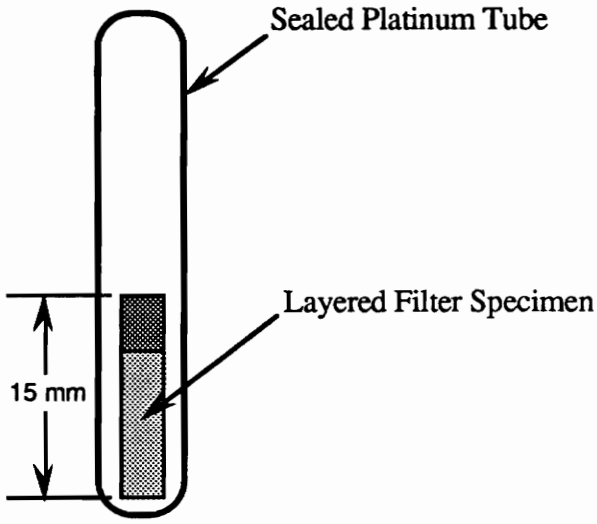

Figure 8. Schematic showing position of layered SiC filter specimen in platinum test chamber.

test set-up (1.5 h) the sample tube remains in a vertical position which causes the section containing the larger grains to come in contact with the alkali solution. These tests were also conducted at temperatures ranging from 700 to 1000°C and pressures ranging from 200 to 1000 psi.

3.4 Sample Evaluation

The morphology of the unexposed and exposed filter samples was determined via scanning electron microscopy (SEM). The SEM was equipped with an energy dispersive X-ray analyzer (EDX) which allowed surface elemental analysis and mapping. The samples were mounted on a carbon stub so that both outer surfaces and interior sections could be scanned. Figure 9 illustrates the manner in which the sample was cut and mounted onto the carbon stubs. The specimens were coated with carbon to prevent charging on the samples. In addition, filter specimens were analyzed using X-ray diffraction methods (XRD). Samples were prepared by grinding the exposed filter specimens with a mortar and pestle. The powdered samples were scanned from 12° to 80° 2Θ.

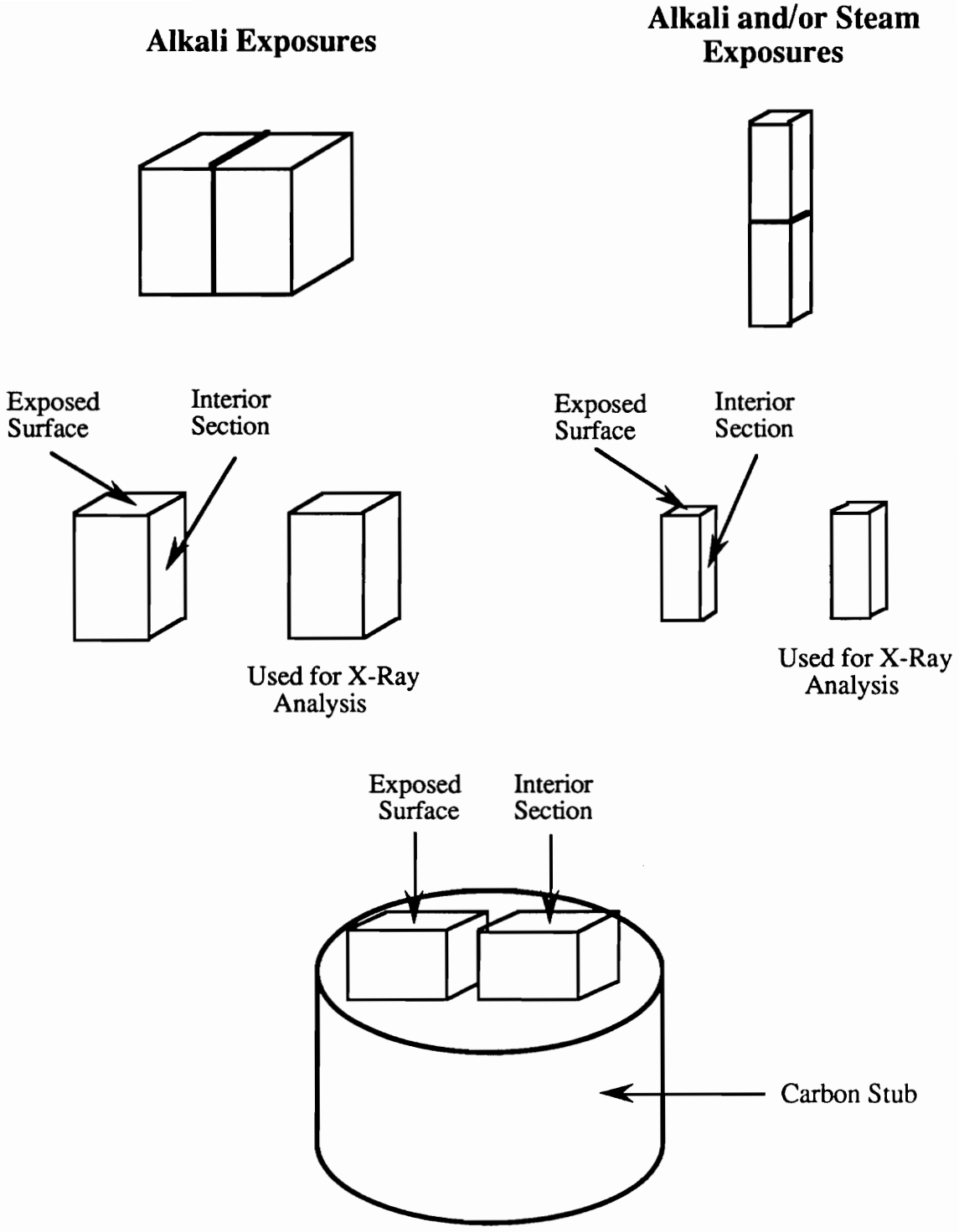

Figure 9. Schematic showing sectioning and mounting of filter specimens.

4. Results and Discussion

4.1 Granular Aluminosilicate

Exposure to High Pressure Steam

Visual observation of the clay-bonded granular aluminosilicate filter specimen showed no physical deterioration other than discoloration following the high pressure steam exposures at 700 - 1000°C and 200 psi. Unexposed specimens of this clay-bonded granular aluminosilicate are sandy-yellow in color, whereas the samples exposed to high pressure steam were greenish-gray in color. XRD analysis of powdered samples showed no changes in mineralogy.

SEM examination of the exterior and fracture surfaces of the exposed aluminosilicate filter showed no signs of deterioration from 700 to 900°C at pressures of 200 and 500 psi compared to that of an unexposed aluminosilicate filter. However, SEM analysis of the sample exposed at 1000°C and 200 psi showed bond melting as in Figure 10. After steam exposures at 1000 psi and temperatures of 700 to 1000°C, the aluminosilicate filter showed deep discoloration and crumbled during handling. SEM examination of filter samples exposed at 500 and 1000 psi at temperatures ranging from 700 to 1000°C showed similar morphology from their 200 psi counterparts.

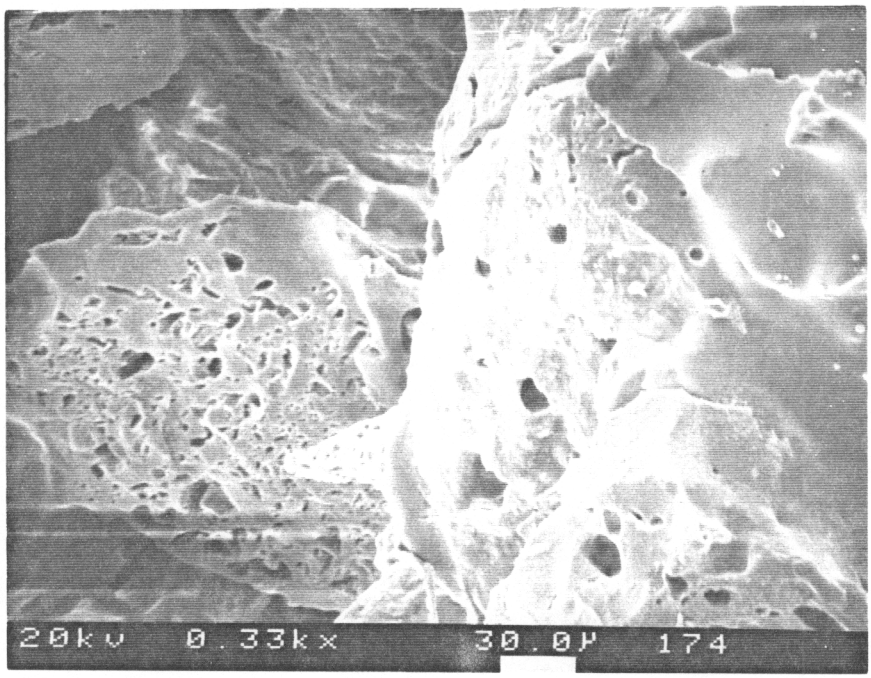

Figure 10. SEM micrograph of clay-bonded, granular aluminosilicate filter exposed to steam at 1000°C for 24 h at 200 psi. Note bond melting. (330X)

Exposure to High Pressure Steam and Alkali

After exposure to sodium and steam at temperatures ranging from 700 to 1000°C and pressures ranging from 200 to 1000 psi, the clay-bonded granular aluminosilicate showed no physical deterioration other than some discoloration (greenish gray to dark gray in color). SEM examination of the exposed filters showed no sign of deterioration at 700°C and all pressures. Bond melting and flowing were observed in samples exposed at 800°C and above. Samples exposed at 800 and 900°C exhibited the formation of spherical particles at the binder-aggregate interface. Figure 11 shows a high magnification SEM micrograph of these spherical particles in the aluminosilicate filter exposed to NaOH and steam at 800°C for 24 h at 200 psi. The spherical particles were likely to be cristobalite (SiO_2) precipitated from the binder phase because EDX analysis indicated that the particles were composed of silicon. More severe degradation of the bonding phase was observed in specimens exposed at 1000°C and 200, 500, and 1000 psi for 24 h. The binder appeared to have melted and then coated the porous surface. Cracking of the aluminosilicate aggregates was also detected in the specimens exposed at 1000°C. Figure 12 is an SEM micrograph which shows bond melting and aggregate cracking after exposure to NaOH and steam at 1000°C for 24 h at 200 psi. EDX analysis of the specimens exposed to steam and alkali revealed that alkali penetrated throughout the specimens. Sodium concentrations of approximately 5% were found in surface and interior sections of all specimens, regardless of the exposure temperatures.

Results from tests conducted with the 5 M KOH solution were similar to those resulting from the NaOH exposures, but the aluminosilicate specimens exposed to KOH solution were more severely degraded. Some spherical cristobalite particles adhered to the aluminosilicate grains in interior as well as surface areas of the samples at temperatures as

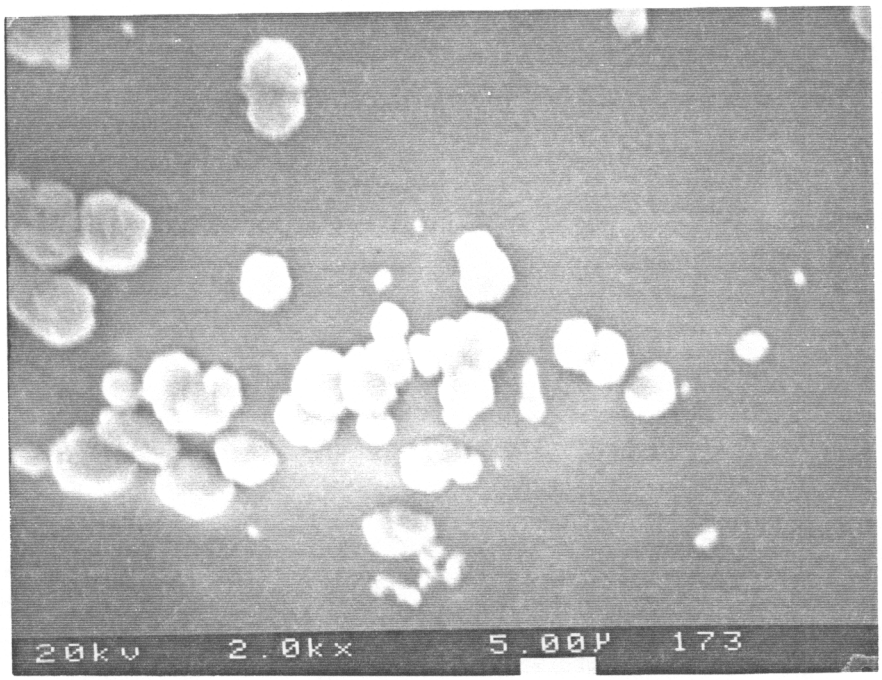

Figure 11. SEM micrograph of clay-bonded granular aluminosilicate filter exposed to steam and NaOH at 800°C for 24 h at 200 psi. Note spherical cristobalite formations. (2000X)

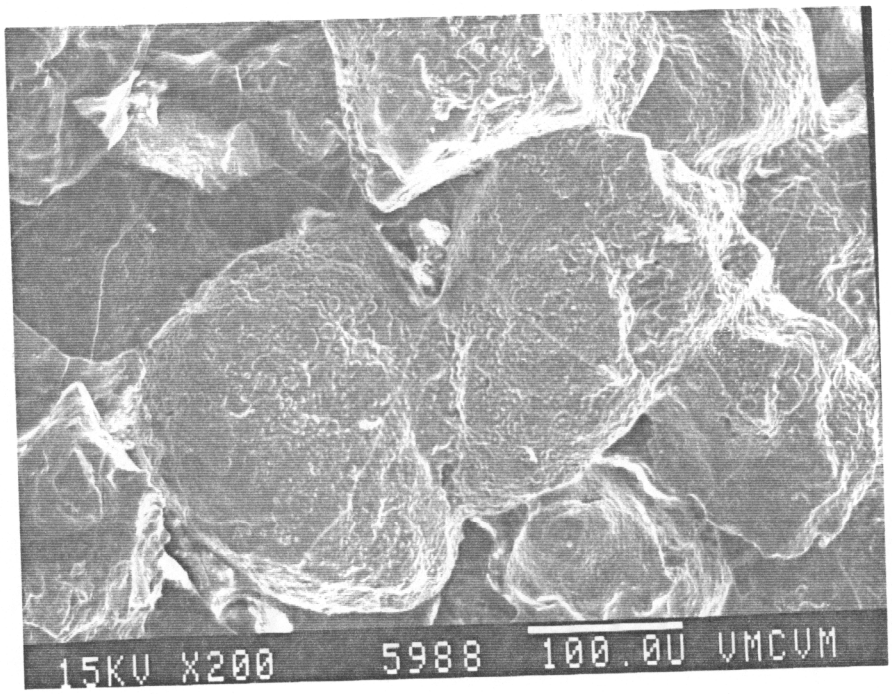

Figure 12. SEM micrograph of clay-bonded granular aluminosilicate filter exposed to NaOH and steam at 1000°C for 24 h and a pressure of 500 psi. Note that the binder phase has coated the aggregates and grain microcracking. (200X)

low as 700°C, and larger amounts of cristobalite were detected by SEM in samples exposed at 800 and 900°C (compared with NaOH). EDX analysis detected 5-15% alkali concentrations throughout the samples, with higher concentrations being detected at portions of the samples which actually came in contact with the alkali solution during test set-up.

4.2 Granular SiC

Exposure to Alkali

The granular SiC filter specimens soaked in alkali and fired at temperatures ranging from 450 to 1000°C showed visual evidence of physical deterioration after exposures to temperatures as low as 700°C. The granular SiC filter developed a glassy coating on its surface after exposures to sodium at 700°C and above. Figure 13 shows the glassy coating which formed on the granular SiC filter after exposure to sodium at 1000°C for 12 h compared to an as-received filter specimen. Based on XRD analysis, SiC was the only compound identified in each specimen, indicating no second crystalline phase formation during exposure to sodium.

SEM examination of the exposed granular SiC filter specimens revealed bond melting and blistering at and near the surface, whereas interior portions of the filter samples appeared unaffected by the alkali exposure. These bond melting and blistering characteristics were detected in samples exposed at 700°C and above. EDX analysis confirmed these observations, showing alkali concentrations ranging from 5% to 10% near the surface and no alkali in interior sections of exposed samples. Figure 14 shows binder melting and flowing which occurred in a granular SiC specimen soaked in NaOH, and fired at 925°C for 12 h.

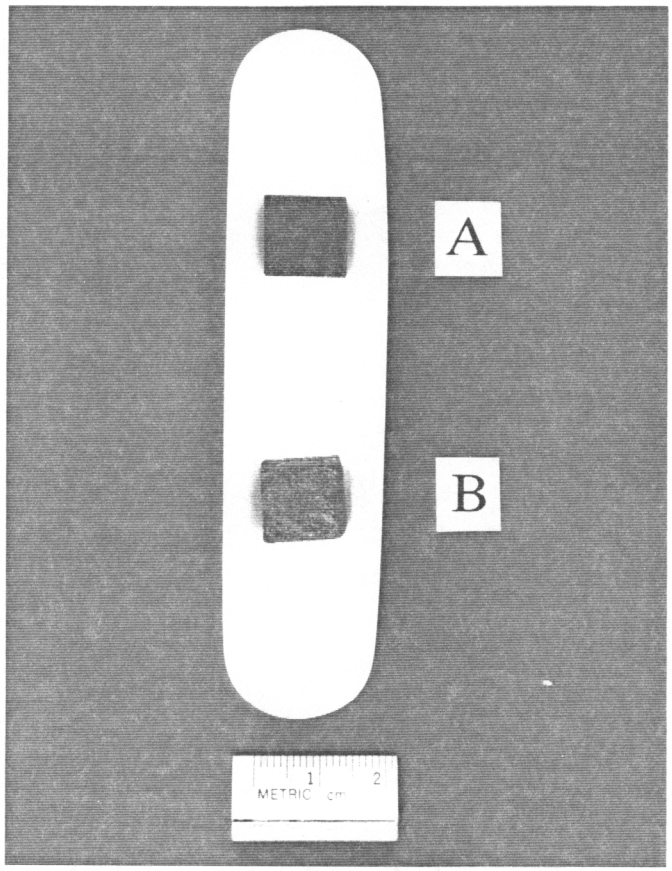

Figure 13. Comparison of as-received and alkali-soaked granular SiC filter. (A) As-received granular SiC filter specimen, (B) granular SiC filter soaked in sodium, dried, and fired at 1000°C for 12 h.

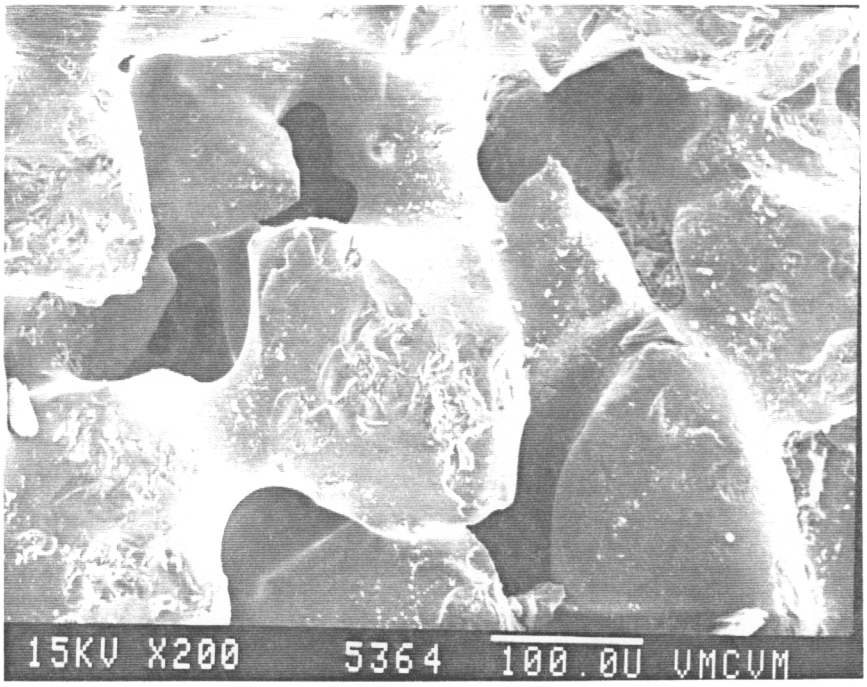

Figure 14. SEM micrograph of granular SiC filter soaked in NaOH, dried, and fired at 925°C for 12 h. Note binder melting, flowing and coating on SiC aggregates. (200X)

After exposures to potassium or potassium/sodium solutions, visual evidence of severe physical deterioration was observed in all specimens. In the specimens exposed to the KOH-NaOH mixture, slight bloating due to bond melting and blistering occurred at temperatures above 800°C. In addition, a glassy coating approximately 0.5 to 1.5 mm thick was noted. The SiC filters were more severely attacked by a 2:1 mixture of KOH-NaOH than by either KOH or NaOH alone. Although all the specimens exhibited a similar glassy or blistered appearance, the KOH-NaOH samples exhibited a bloated appearance and degradation throughout the sample. Figure 15 shows the blistering which occurred during a 1000°C, 12 h exposure of the specimen soaked in a 2:1 mixture of KOH and NaOH. SEM examination showed bond melting and bubbling (Figure 16), and EDX indicated trace amounts of sodium and potassium within the interior of the filter specimen. However, SEM analysis indicated that specimens exposed to potassium alone did not exhibit alkali attack in the center of the filter specimens, nor was alkali detected by EDX analysis.

The visual appearance of the granular SiC candle specimens exposed at 925°C and 1225°C to alkali vapor produced by evaporation of either Na_2CO_3 or K_2CO_3 was comparable to that of filter specimens soaked in a saturated alkali solution and fired at similar temperatures. The edge of each specimen located closest (approximately 2 cm) to the alkali source showed severe attack, and there appeared to be little or no attack at the outer edge of each sample located approximately 3 cm from the alkali source (Figure 17). Samples shown in this figure were exposed to Na_2CO_3 at 1225°C for 20 h.

After exposure to alkali vapors, the filter specimens had a slightly bloated, glassy coating. SEM and EDX analysis of the granular filter indicated that alkali penetration was less in specimens exposed to alkali vapor than in specimens soaked in alkali solutions prior

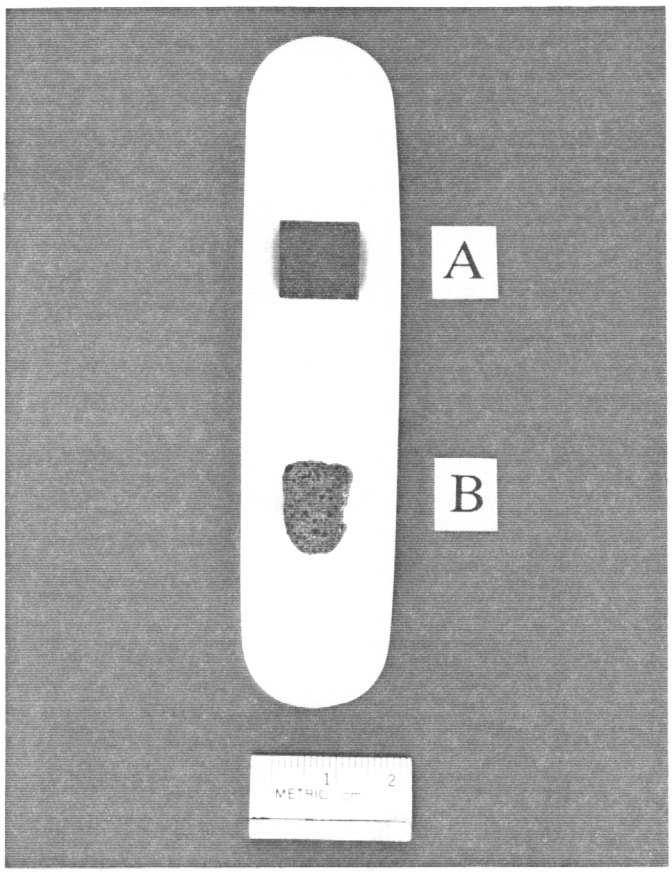

Figure 15. Comparison of as-received and alkali-soaked granular SiC filter. (A) As-received granular SiC filter specimen, (B) granular SiC filter specimen exposed to 2:1 mixture of KOH and NaOH for 12 h at 1000°C. Though the exposed specimen looks smaller than the unexposed filter, blistering and severe volume expansion occurred making it necessary to break the specimen for removal from the alumina combustion boat.

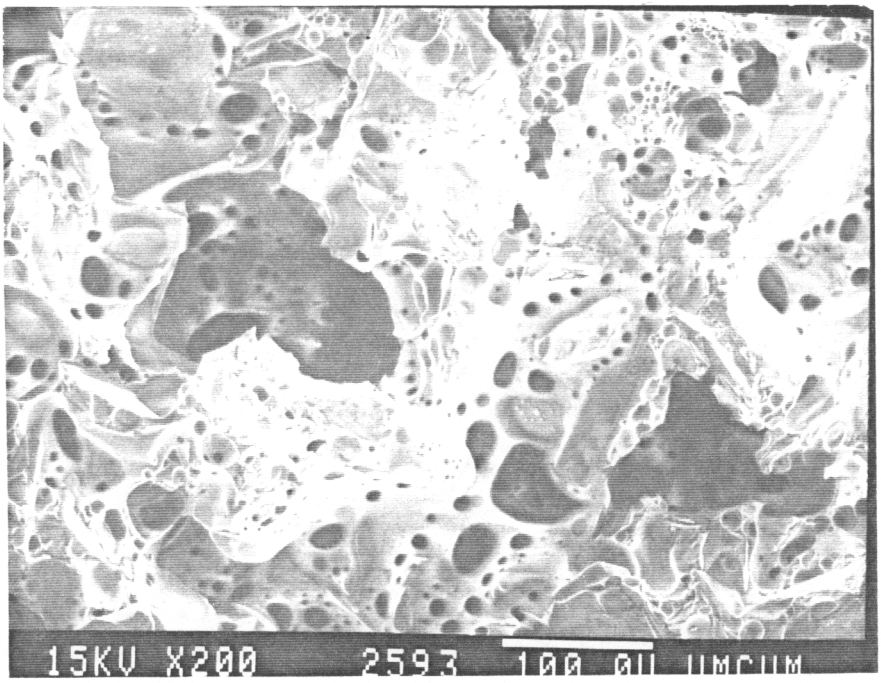

Figure 16. SEM micrograph of the granular SiC filter soaked in a 2:1 mixture of KOH and NaOH, dried, and fired at 700°C for 12 h. Note bond melting and bubbling. (200X)

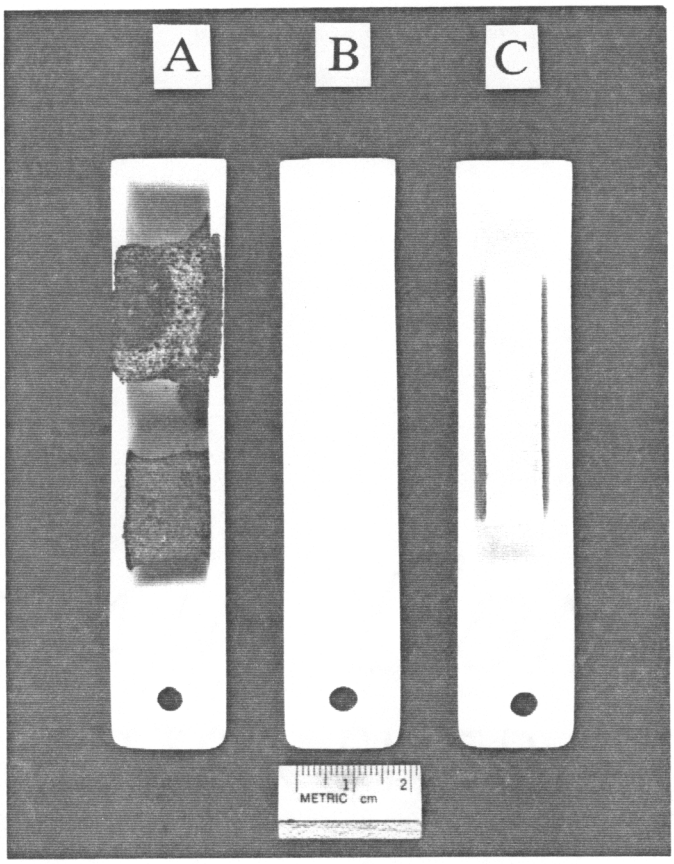

Figure 17. Arrangement of SiC filter specimens and kaolinite bars in furnace. (A) Exposed membrane SiC filter (top) and exposed granular SiC filter (bottom), (B) crucible containing K_2CO_3, (C) exposed kaolinite bar with glazed surface. Exposure conditions: K_2CO_3 at 1225°C for 20 h.

to exposure. EDX indicated the presence of little or no alkali in the interior of the samples; however, exposed surfaces were slightly bloated and contained 2-3% alkali. SEM examination of the granular specimens revealed a blistered, glass-like network covering the specimen surfaces. It was also found that specimens exposed to K_2CO_3 vapors were more severely attacked than samples exposed to Na_2CO_3 vapors.

The SiC aggregates in the granular SiC filter showed strong resistance to alkali attack; that is the aggregates retained as-received morphology and the grains contained no detectable alkali. Using EDX, it was found that sectioned SiC grains contained no alkali. Even at the surface of the SiC aggregates coated with binder, EDX indicated the presence of little or no alkali.

Exposure to High Pressure Steam

Visual inspection of granular SiC filter specimens exposed to high pressure steam revealed no noticeable deterioration at 700 - 1000°C and a pressure of 200 psi for 24 h. However, SEM examination of these samples revealed that the binder phase flowed at all temperatures, with the degradation increasing with increasing temperature. In the samples exposed at 1000°C and pressures of 200, 500, and 1000 psi for 24 h, small deposits were noted on the surface of the SiC grains. There appeared to be several hundred spherical deposits ranging from 1-10 μm clinging to the grains, whereas only a few could be detected in the binder phase. EDX spectra identified the spherical particles as predominantly silicon. Analysis by XRD of the specimens exposed at 1000°C for 24 h revealed an increase in the amount of cristobalite when compared to unexposed samples, suggesting that the SiC grains were oxidized in the steam atmosphere. SEM analysis revealed no difference between the specimens exposed to high pressure (500 and 1000 psi)

and their low pressure counterparts (200 psi).

Exposure to High Pressure Steam and Alkali

After exposure to the NaOH solution at 700 to 1000°C and pressures of 200-1000 psi, the granular SiC samples appeared to be somewhat bloated, especially where portions of the sample came in contact with the alkali solution. Samples exhibited similar bloating following exposures to the KOH solution at 700 to 1000°C and pressures of 200-1000 psi. SEM examination of samples exposed to the alkali solutions showed that blistering due to bond melting and oxidation of the SiC grains occurred throughout the interior section of the filter specimens at all temperatures. Moreover, the pores at the exposed surface were sealed by the binder which had melted and flowed. The binder appeared to have migrated to and coated the surface as evidenced by EDX analysis revealing decreased amounts of Al_2O_3 in the interior sections and increased Al_2O_3 contents at the outer surfaces. Figures 18 and 19 illustrate the blistering characteristics of the interior sections and the pore sealing of the surface. Also found in the interior section of the filter specimens were spherical cristobalite grains protruding from the SiC aggregates. These cristobalite beads were present at temperatures as low as 700°C and in much greater quantities than those of the granular SiC specimens exposed to steam alone. Binder depletion was also noted in the samples exposed to the alkali solution. Degradation increased with increasing temperature, and the sample exposed to 1000 psi crumbled during handling. SEM examination of the granular SiC specimens exposed to the KOH solution revealed similar but somewhat greater alkali/steam attack than the specimens exposed to NaOH. SEM analysis revealed no difference between the specimens exposed to high pressure (500 and 1000 psi) and their low pressure counterparts (200 psi).

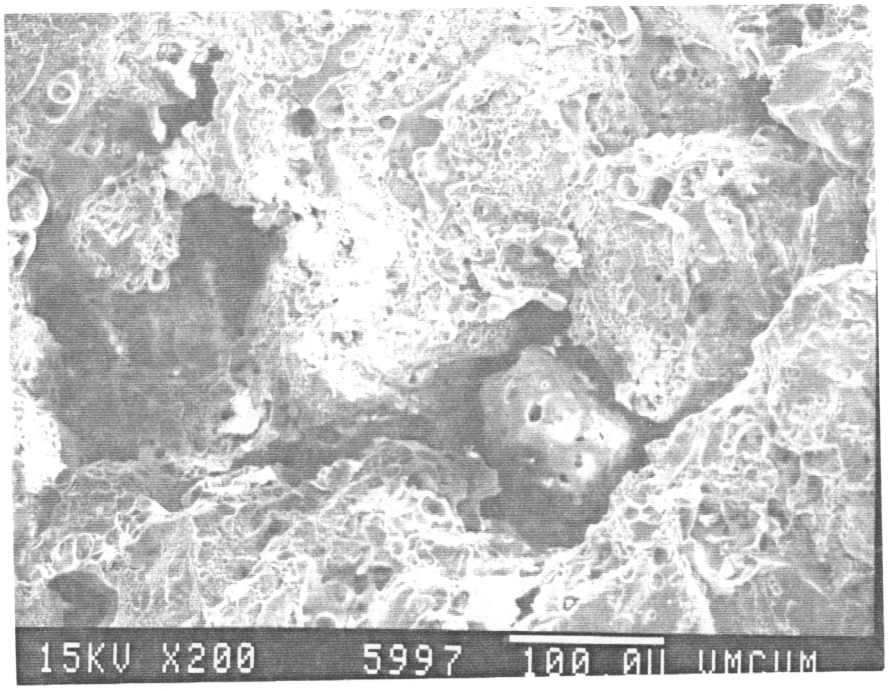

Figure 18. SEM micrograph of interior section of clay-bonded granular SiC filter exposed to KOH and steam at 900°C for 24 h at 200 psi. Note bond melting and blistering. (200X)

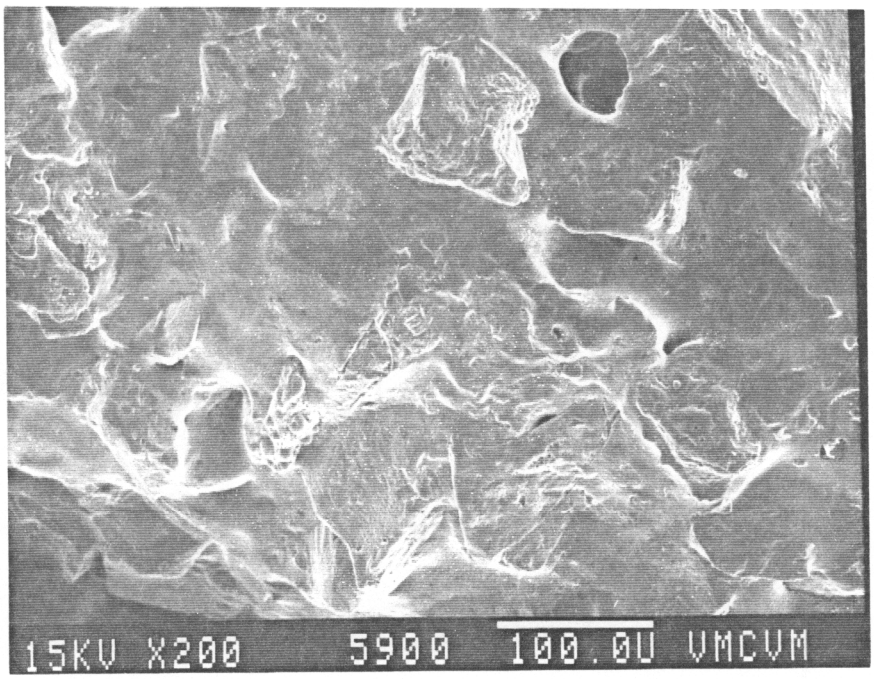

Figure 19. SEM micrograph of exterior section of clay-bonded granular SiC filter exposed to KOH and steam at 800°C for 24 h at 200 psi. Note bond flowing and pore sealing. (200X)

4.3 Layered SiC

Exposure to Alkali

The layered SiC filter specimens soaked in alkali and fired at temperatures ranging from 450 to 1000°C showed visual evidence of physical deterioration after sodium exposures to temperatures as low as 700°C. According to XRD analysis, SiC was the only compound identified in all specimens, indicating no second crystalline phase formation.

Layered SiC filter specimens suffered severe volume expansion from bond melting. Bubbling due to the escape of gaseous reactant products was also observed. Figure 20 shows the bloated appearance of the layered filter compared to its as-received counterpart. The smaller grained area suffered the most severe volume expansion due to a higher surface area. SEM examination and EDX analysis indicated deep sodium penetration, and only at the center of the layered SiC sample did the aggregates and binder material retain the same appearance as the unexposed filter. SEM analysis revealed bond melting. Figure 21 shows blistering of a layered SiC filter specimen soaked in the NaOH solution, dried and fired at 700°C for 12 h. Alkali concentrations of 8 - 11% were detected on the surface of the exposed samples, with decreasing alkali concentrations as the center of the sample was approached.

After exposure to potassium and potassium/sodium solutions, layered SiC samples fired at 450-1000°C showed visual evidence of severe physical deterioration. In the specimens exposed to the potassium/sodium mixture, bloating from bond melting occurred at temperatures above 800°C, and specimens showed blistering, small cracks and pieces broken from the surface. Although severe bloating did not occur in filters which were exposed to potassium, specimens exposed at 800 °C and above had a thick glassy coating of approximately 0.5 to 1.5 mm. Visual observation and SEM analysis of exposed

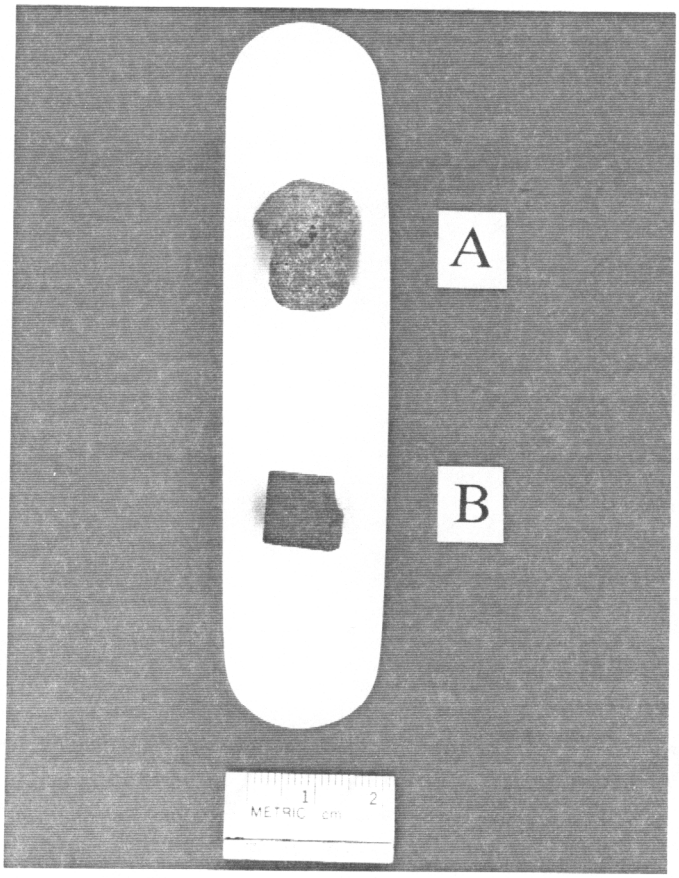

Figure 20. Comparison of as-received and alkali-soaked layered SiC filter. (A) layered SiC filter specimen soaked in sodium, dried, and fired at 700°C for 12 h. Note severe volume expansion in smaller grained area, (B) As-received granular SiC filter with an outer layer of small aggregates.

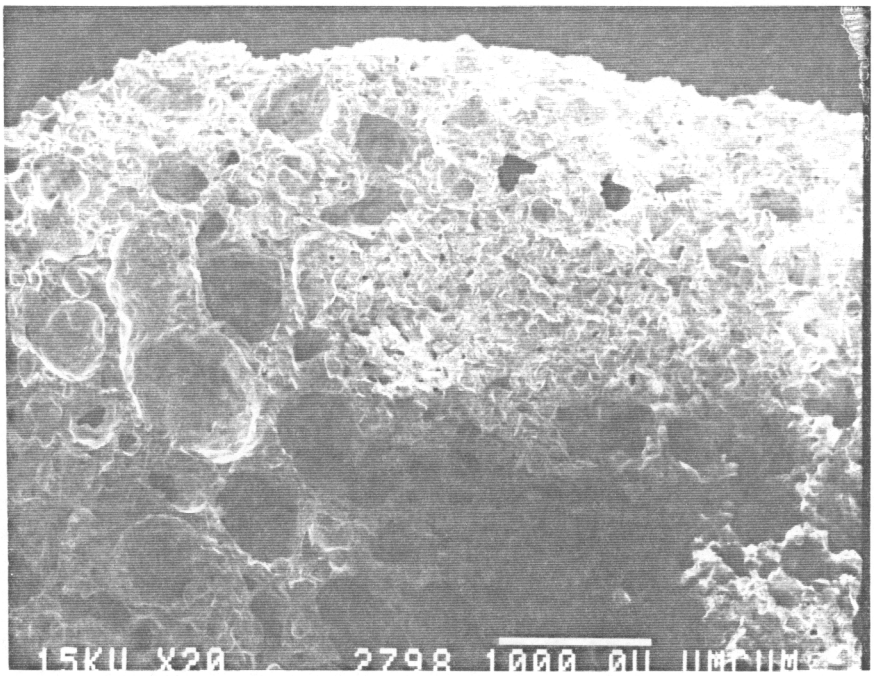

Figure 21. Low magnification SEM micrograph of granular SiC filter soaked in sodium, dried, and fired at 1000°C for 12 h. Note volume expansion and bubbled voids. (20X)

specimens indicated that the SiC filters are more severely attacked by a 2:1 mixture of KOH-NaOH than by either KOH or NaOH alone. SEM examination showed bond melting and severe blistering, and EDX indicated trace amounts of sodium and potassium within the interior of the filter specimen. However, SEM and EDX analyses indicated that alkali did not penetrate to the center of the specimens exposed to potassium alone, and the alkali attack was less severe than samples exposed to the KOH-NaOH mixture.

Exposure to High Pressure Steam and Alkali

After exposures to the NaOH solution at 700 - 1000°C and pressures of 200 - 1000 psi, the section of the layered SiC sample which came in direct contact with the alkali solution was coated with a glassy phase which had flowed and coated the outer surface. The samples exhibited similar glazing following exposure to a KOH solution for 24 h at 700° to 1000°C and a pressure of 200 psi.

SEM examination of interior portions of the layered SiC samples exposed to the NaOH solution revealed that bond melting had occurred throughout the samples at all temperatures. The formation of spherical particles, 1-10 μm in diameter, on the SiC grains was also observed. XRD analysis of the filter specimens showed that a small amount of SiC in the specimens had reacted to form cristobalite. The exterior surfaces showed more extreme attack than interior sections, especially on the glazed areas of the sample. Figure 22 shows bond melting and blistering near the surface of a specimen which was exposed to NaOH and steam at 700°C for 24 at 200 psi. EDX analysis detected sodium concentrations of 1-2 % at the surface and only trace amounts in the interior sections. Also, higher concentrations of alkali (3-5 %) were detected on the glazed areas. The increase in alkali/steam attack with increasing temperature observed in previous tests of the granular

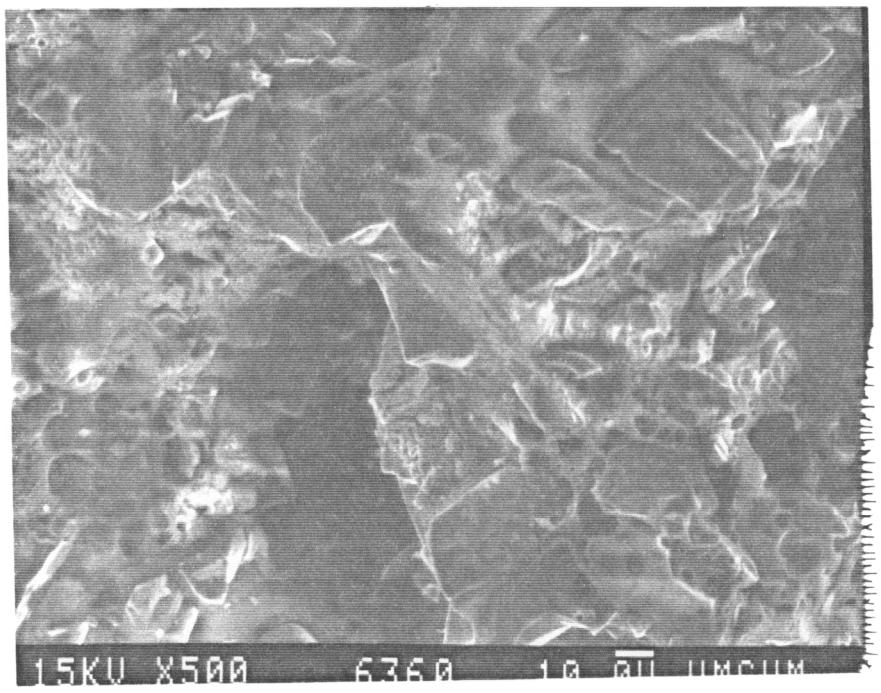

Figure 22. SEM micrograph of small aggregates on outer surface layered, granular SiC filter exposed to NaOH and steam at 700°C for 24 h at 500 psi. Note bond melting and bubbling. (500X)

and membrane SiC candles and the aluminosilicate candle was not observed in the layered SiC specimen.

SEM examination of the layered SiC specimens exposed to the KOH solution revealed similar, but somewhat greater alkali/steam attack than the specimens exposed to NaOH. Similar binder melting and flowing was noted as well as the presence of the spherical particles on the SiC grains. SEM analysis revealed no difference in morphology between the specimens exposed to high pressure (500 and 2000 psi) and their low pressure counterparts (200 psi).

4.4 Membrane SiC

Exposure to Alkali

The membrane SiC filter specimens soaked in alkali solutions of NaOH and fired at temperatures ranging from 450 to 1000°C showed visual evidence of physical deterioration after exposures to temperatures as low as 700°C. Although a thick glassy coating was observed on the membrane SiC specimens, severe bloating did not occur and SiC was the only compound identified in each specimen. SEM examination showed degradation of the filters from bond melting and blistering which decreased toward the center of the sample. The fibrous membrane appeared to have prevented deep sodium penetration within the specimen.

After exposures to potassium and potassium/sodium solutions, visual evidence of severe physical deterioration in all specimens was observed. SEM examination showed bloating from bond melting as well as blistering due to the escape of gaseous reactant products in the specimens exposed to the potassium/sodium mixture at temperatures above 800°C. The KOH-NaOH impregnated samples were much more severely bloated, often

showing small cracks and pieces broken from the surface, and exhibited attack throughout the sample. Although severe bloating did not occur in filters which were exposed to potassium, specimens exposed at 800 °C formed a thick glassy coating approximately 1 to 2 mm thick. Visual observation of the exposed specimens indicated that the SiC filters are more severely attacked by a 2:1 mixture of KOH-NaOH than by either KOH or NaOH alone. At the centers of the membrane SiC samples, the bond and grain structure appeared unaffected, and EDX did not indicate the presence of potassium.

The visual appearance of the specimens exposed at 925°C and 1225°C to alkali vapor produced by evaporation of either Na_2CO_3 or K_2CO_3 was comparable to that of membrane SiC filter specimens soaked in a saturated alkali solution and fired at similar temperatures. The outer fibrous membrane of the filter showed extreme volume expansion when compared to its interior region and to other filter types. It should be noted that the membrane reacted more severely in the K_2CO_3 environment than the Na_2CO_3 environment. The edge of the specimen located closest to the alkali source (approximately 2 cm) showed the most attack, and there appeared to be little or no attack at the outer edge located approximately 3 cm from the alkali source (Figure 17).

EDX analysis indicated little or no alkali in the interior of the samples, 10-15% alkali on the bloated membrane and 2-3% alkali on the surfaces not covered by the membrane. At the membrane surface, SEM examination revealed the formatiom of a bubbly, glass-like network (Figure 23) due to membrane-alkali interaction. Broken SiC grains were dispersed in a glassy network at the surface due to the severe volume expansion of the membrane. Some binder depletion was noted below the surface while the binder could not be distinguished from other constituents at the surface due to binder melting. Interior sections showed that SiC grains and binder were intact (Figure 24).

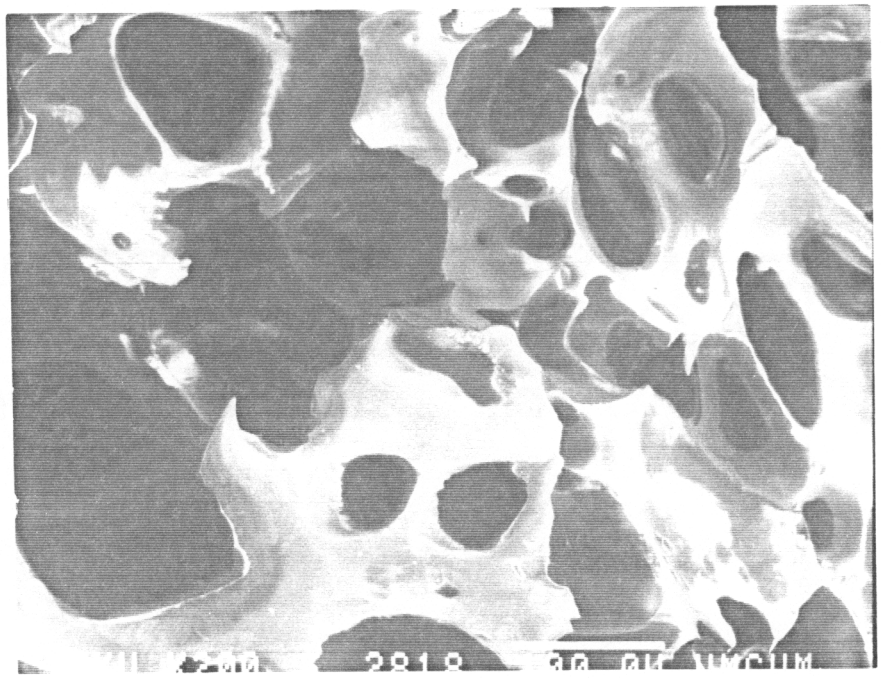

Figure 23. SEM micrograph of outer surface of membrane SiC filter after exposure to K_2CO_3 vapors for 24 h. Note glassy network of bubbles. (200X)

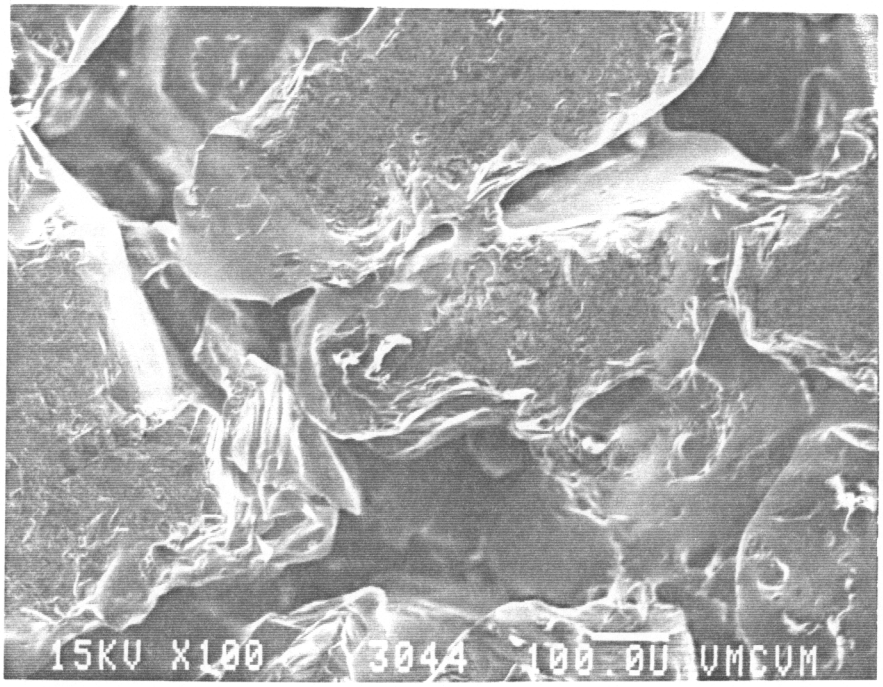

Figure 24. SEM micrograph of interior section of membrane SiC filter after exposure to K_2CO_3 vapors at 1225°C for 24 h. Note the as-received morphology and no binder melting, flowing, or depletion in interior section. (100X)

The KOH-NaOH impregnated samples were much more severely bloated, often showing small cracks and pieces broken from the surface, and exhibited attack throughout the sample.

Exposure to High Pressure Steam

There was no visible physical deterioration of the membrane SiC filter specimens after exposure to high pressure steam (200-1000 psi) at 700 - 1000°C for 24 h, and XRD analysis of exposed samples showed no changes in mineralogy. However, SEM examination revealed that bond melting and flowing had occurred at 700°C and 200 - 1000 psi. Blistering was detected in specimens exposed at 700°C and 200 psi, whereas other areas appeared unaffected by steam exposure. As the exposure temperature was increased the areas of blistering became more prevalent. Cristobalite was detected at the SiC grains of specimens exposed at 1000°C, suggesting oxidation of the SiC aggregates. Figure 25 shows the morphology of the membrane SiC filter after exposure to steam at 900°C and 200 psi for 24 h. Binder phase melting and flowing were detected, as was blistering in certain areas. SEM analysis revealed no difference between the specimens exposed to high pressure (500 and 1000 psi) and their low pressure counterparts (200 psi).

Exposure to High Pressure Steam and Alkali

After exposures to the alkali-steam atmospheres, the filter membranes showed visual deterioration at approximately 900°C. A glassy coating was observed on the membrane samples exposed at 900 and 1000°C. SEM analysis indicated that the aluminosilicate fibers of the membrane sintered in the specimens exposed at 700 and

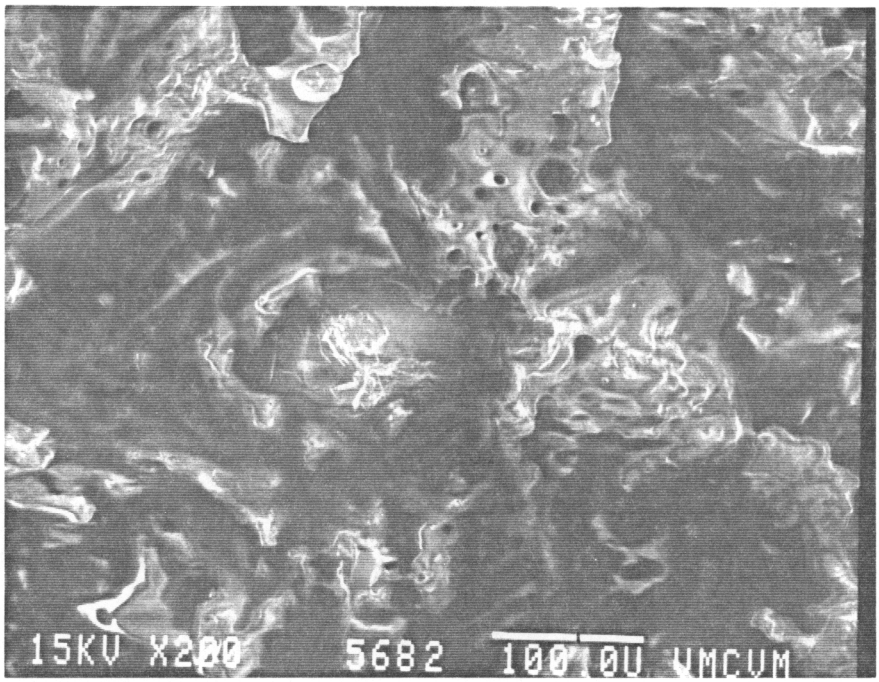

Figure 25. SEM micrograph of membrane SiC filter exposed to steam at 900°C for 24 h at 200 psi. Note bond melting and flowing. (200X)

800°C, whereas those samples exposed to alkali and steam at 900 and 1000°C showed fiber melting which formed a glassy network.

Following exposures to the NaOH-steam atmospheres at all temperatures the specimens were found to be broken into several pieces. The pieces which came in direct contact with the alkali solution appeared to be somewhat bloated. SEM examination of interior portions of the exposed samples indicated that changes had occurred throughout the microstructure of the samples at temperatures as low as 700°C for 24 h. Blistering of the binder phase was detected in isolated sections of the sample. Although some areas appeared unaffected, analysis by EDX showed alkali concentrations of 3-5% throughout the sections which came in direct contact with the alkali solution, and concentrations of 2-3% in the remaining pieces exposed at 700 °C. Unidentified particles were intermingled with the binder phase. EDX analysis of the particles revealed an unusually high amount of sodium (22%). Similar bond melting and unidentified particles were observed throughout the broken sections of the samples exposed at 800 and 900°C.

The most severe alkali attack was noted in the filter specimen exposed at 1000°C for 24 h. The melted binder flowed and coated the outer surface of the broken sample fragments indicating that breakage occurred early in the test period. Bubbling due to vaporization was more prominent in the sample exposed at 1000°C, especially in those pieces which came in direct contact with the alkali solution. Cristobalite formation occurred in membrane SiC samples exposed at 800, 900, and 1000°C (Figure 26). EDX analysis showed 5-7% alkali concentrations throughout the fragments which came in direct contact with the NaOH solution, and concentrations of 3-4% alkali throughout the remaining fragments.

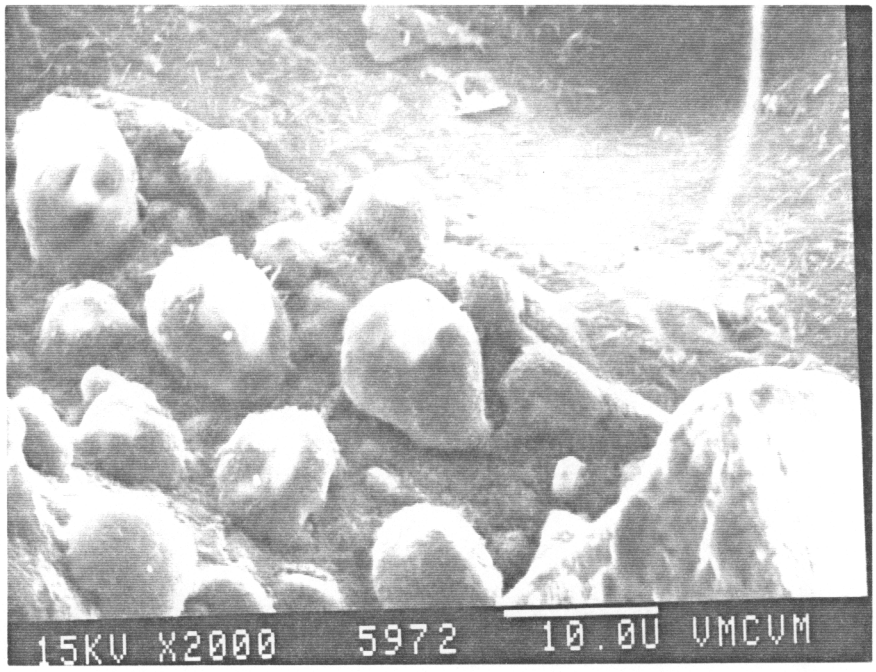

Figure 26. SEM micrograph of the membrane SiC filter exposed to NaOH and steam at 800°C for 24 h at 200 psi. Note the formation of cristobalite beads. (2000X)

The observed physical deterioration of the membrane SiC filter specimens following exposures to the KOH-steam atmospheres was similar to that observed previously in the NaOH-steam atmospheres. Upon removal from the platinum tube, the samples were found to be broken into several pieces. Analysis by EDX showed alkali concentrations of 3-5% throughout the samples. Unidentified particles, similar to those found in the NaOH-steam exposures, were intermingled with the binder phase. EDX analysis of the particles revealed high concentrations of potassium (18%). Bond melting, bubbling, and unidentified particles were observed in samples exposed at 800, 900, and 1000°C, with the most severe attack occurring at 1000°C. SEM analysis revealed no difference between the specimens exposed to high pressure (500 and 1000 psi) and their low pressure counterparts (200 psi).

4.5 Comparison of Filters

Results from the alkali exposure tests indicated that the commercial SiC candle filters are susceptible to alkali attack. SiC specimens soaked in alkali solutions and exposed to alkali vapors exhibited glazing and severe volume expansion. The granular SiC filter was found to be the most resistant to alkali attack, though severe degradation occurred at temperatures as low as 700°C. Volume expansion of the granular filter was not as severe as that of the membrane filter. Though the membrane SiC filter exhibited less alkali penetration than the granular SiC filter, the surface membrane was severely bloated and pore sealing occurred. The layered SiC filter suffered from severe volume expansion especially in the outer layer of small grains (higher surface area) and appeared to be the most severely attacked by alkali.

SiC filter specimens soaked in a 2:1 mixture of KOH to NaOH, dried and, fired at

high temperatures were more severely corroded than samples exposed to KOH or NaOH alone. Also, it was found that SiC specimens exposed to a KOH solution were slightly more corroded than specimens exposed to a NaOH solution. SiC filter specimens exposed to Na_2CO_3 or K_2CO_3 vapors exhibited degradation similar to alkali-soaked specimens, but the degradation was less severe.

It was also found that commercial ceramic candle filters are susceptible to degradation in high pressure, high temperature steam environments. Of the four filters exposed to steam environments it was determined that the clay-bonded granular aluminosilicate candle filter appears to be the most corrosion resistant, though degradation occurred at temperatures as low as 800°C. Cristobalite was detected in the SiC filters exposed to high pressure steam, whereas the aluminosilicate filter contained none.

Cristobalite also formed in the aluminosilicate filter during exposure to steam and alkali at 1000°C, whereas the SiC filters formed cristobalite at 700°C and above. The spherical cristobalite growths were similar to those detected in SiC specimens exposed to steam alone, but they were present at lower temperatures (700°C) and in greater quantities. The tendency of the SiC filters to form cristobalite during exposure to steam and steam/alkali environments would suggest that steam enhances the degradation of the SiC aggregates. The formation of high expanding cristobalite can result in strength degradation of the candle filters.

After exposures at pressures of 500 and 1000 psi and temperatures ranging from 700 to 1000°C, the aluminosilicate and SiC filter specimens revealed steam attack similar to that shown by their filter counterparts exposed at a pressure 200 psi. It was therefore concluded that below 1000 psi pressure appears to have no effect on the degree of steam attack.

5. Conclusions

1. Commercial candle filters are susceptible to degradation in alkali and steam-containing environments.

2. Of the three types of SiC filters, the granular SiC filter was found to be the most resistant to alkali attack.

3. A mixture of potassium and sodium is more corrosive to commercial candle filters than either sodium or potassium alone; potassium is more corrosive than sodium.

4. Of the four filters exposed to high pressure steam environments, the clay-bonded granular aluminosilicate candle filter appears to be the most corrosion resistant.

5. Increased temperature will enhance filter degradation, whereas increased pressure (to 1000 psi) appears to have no effect on the degree of alkali and steam attack.

6. Corrosion caused by alkali coupled with steam is much more severe than corrosion caused by either alkali or steam alone.

6. References

1. J. Sawyer, "Assessment of the Causes of Failure of Ceramic Filters for Hot Gas Clean-up in Fossil Energy Systems and Determination of Materials Research and Development Needs, "Oak Ridge National Laboratory, Oak Ridge, Tennessee, January, 1989.

2. J. Sawyer, R.J. Vass, N.R. Brown, and J.J. Brown, "Corrosion and Degradation of Ceramic Particulate Filters in Direct Coal-Fired Applications," Paper presented at the International Gas Turbine and Aeroengine Congress and Exposition, Brussels, Belgium, June 11-14, 1990.

3. "Performance of Porous Sintered Ceramic Filters," Materials and Components in Fossil Energy Applications, U.S. Department of Energy Newsletter, DOE/FE-0080/80, Oak Ridge Operations, June 1, 1989.

4. J.E. Oakey and G.P. Reed, "Behavior of High Temperature Filter Materials in Hot Gasifier and Combustor Gas Applications," High Temperature Technology, Vol. 5, No. 4, 1987, pp. 171-180.

5. D.R. Dierks and D. Stahl, "A Review of Refractory Materials for the Memphis Industrial Fuel Gas Demonstration Plant," ANL/FE-81-60, Argonne National Laboratory, Argonne, Illinois, September 1981.

6. C.R. Kennedy, "Alkali Attack on a Mullite Refractory in the Grand Forks Energy Technology Center Slagging Gasifier," Journal of Materials for Energy Systems, Vol. 3, No. 1, June, 1981, p. 27.

7. R.F. Hayden, "Study of the Resistance of Refractories to Alkali Vapors," Master's Thesis, Virginia Polytechnic Institute and State University, May 1976.

8. R.E. Farris and J.E. Allen,"Aluminous Refractories Alkali Reactions," Iron and Steel Engineer, Vol. 50, No. 2, 1973, pp. 67-74.

9. C.R. Rigby and R. Hutton, "Action of Alkali and Alkali-Vanadium Oxide Slags on Alumina-Silica Refractories," Journal of the American Ceramic Society, Vol. 45, No. 1, pp. 68-73, 1962.

10. G.C. Wei, V.J. Tennery, and L.A. Harris, "Effects of Alternate Fuels, Report No.1, Analysis of High-Duty Fireclay Refractories Exposed to Coal Combustion," ORNL/TM-5909, Oak Ridge National Laboratory, Oak Ridge, TN, December 1977.

11. P.H. Havranek, "Alkali Attack on Blast Furnace Refractories," Journal of British Ceramic Society Transactions, Vol. 77, No. 3, 1978, pp. 92-97.

12. T.E. Easler, "Corrosion Behavior and Mechanical Properties of Silicon Carbide Exposed to Coal Gasification Environment," ANL/FE-84-21, Argonne National Laboratory, Argonne, IL, June 1985

13. E.A. Gulbransen and S.A. Jansson, "The High Temperature Oxidation, Reduction and Volatilization Reactions of Silicon and Silicon Carbide," Oxidation of Metals, Vol. 4, No. 3, 1972, pp. 181-201.

14. C. Wagner, "Passivity During the Oxidation of Silicon at Elevated Temperatures," Journal of Applied Physics, Vol. 29, No. 9, 1958, pp. 1295-1297.

15. J.W. Hinze and H.C. Graham, "The Active Oxidation of Si and SiC in the Viscous Gas-Flow Regime," Journal of the Electrochemical Society,Vol. 123, No. 7, 1976, pp. 1066-1073.

16. D.S. Fox, N.S. Jacobson and J.L. Smialek, "The Molten Salt Corrosion of SiC and Si_3N_4," Structural Ceramics, May 1986, Workshop Help in Cleveland Ohio, sponsored by NASA, Washington, D.C.

17. N.S. Jacobson and J.L Smialek, "Hot Corrosion of Sintered α-SiC at 1000°C," Journal of the American Ceramic Society, Vol. 68, No. 8, pp. 432 -39, 1985.

18. J.L. Smialek, D.S. Box, and N.S. Jacobson, "Hot Corrosion Attack and Strength Degradation of SiC and Si_3N_4," NASA/89820, April, 1987.

19. M.S. Crowley, "Hydrogen Steam Reactions in Refractories," Paper presented at the 76th Annual Meeting of the American Ceramic Society, April 30, 1974 (Refractories Division).

20. R.E. Dial, "Refractories for Coal Gasification and Liquefaction," Ceramic Bulletin, Vol. 54, No. 7, 1975, pp. 640-643.

21. L.Y. Sadler, III, H. Heystek, N.S. Raymon, and T.A. Clancy, "Refractories for Dry Ash Coal Gasifiers," Bureau of Mines Report of Investigations 8913, 1984.

22. L.Y. Sadler, III, and E.G. Davis, "Steam-Induced Volatilization of Silica from Refractories," U.S. Bureau of Mines Report of Investigations 9052, 1986.

23. F.L. Horn, J.A. Fillo, and J.R. Powell, "Performance of Ceramic Materials in High Temperature Steam and Hydrogen," Journal of Nuclear Materials, Vol. 85 and 86, Part A, 1979, pp. 439-443.

24. A.J. Hayes et. al., Eds., R.E. Tressler, J.A. Costello and Z. Zheng, "Oxidation of Silicon Carbide Ceramics," Industrial Heat Exchangers, Vol. 6, 1985, pp. 307-314.

25. J.I. Federer, "Corrosion of Materials by High Temperature Industrial Combustion Environments - A Summary," ORNL/TM-9903, February, 1986.

7. Vita

Jean Miller was born in Bainbridge, Maryland on March 31, 1967, the daughter of Jacob C. and Daphne E. Miller. She received her high school education at Greenbrier East High School in Fairlea, West Virginia. She entered Virginia Polytechnic Institute and State University in the Fall of 1985 where she received a Bachelor of Science degree in Materials Engineering in the Spring of 1989. As an undergraduate Jean was a Resident Advisor and was involved in Alpha Phi Omega, a National Co-ed Service Fraternity. She continued her education by entering the graduate program at Virginia Polytechnic Institute and State University in the Fall of 1989. She completed the requirements for a Master of Science in Materials Engineering in May 1991

She is a member of the American Ceramic Society as well as ASM International at Virginia Polytechnic Institute and State University.